MASTER EN SCIENCES CHIMIQUE À FINALITÉ APPROFONDIE

Single Walled Carbon Nanohorns- and Single Walled Carbon Nanotubes-Based Catalysts for the Conversion of Carbon Dioxide

Ryabov, Alexey

Award date:
2019

Awarding institution:
Universite de Namur

UNIVERSITÉ DE NAMUR

Faculté des Sciences

SINGLE WALLED CARBON NANOHORNS- AND SINGLE WALLED CARBON NANOTUBES-BASED CATALYSTS FOR THE CONVERSION OF CARBON DIOXIDE

Mémoire présenté pour l'obtention

du grade académique de Master Chimie «Chimie du Vivant et des Nanomatériaux» : Finalité Approfondie

Alexey Ryabov

Janvier 2019

UNIVERSITÉ DE NAMUR
Faculté des Sciences
Secrétariat du Département de Chimie
Rue de Bruxelles 61 – 5000 NAMUR
Téléphone : +32(0)81 72.54.44 – Téléfax : +32(0)81 72.54.40
E-mail : enseignement.chimie@unamur.be - www.unamur.be/sciences

Single Walled Carbon Nanohorns- and Single Walled Carbon Nanotubes-Based Catalysts for the Conversion of Carbon Dioxide

Alexey Ryabov

Résumé

De nos jours, la source principale d'énergie provient des combustibles fossiles. Un des sous-produits dans le processus de combustion est le dioxyde de carbone (CO_2). Ces dernières années, le développement de nouveaux procédés basés sur la conversion du CO_2 reçoit beaucoup d'attention. La raison est la possibilité de transformer un déchet en un réactif abondant, renouvelable et facilement disponible en produits utiles.

Les carbonates cycliques, synthétisés par la réaction du dioxyde de carbone et des époxydes, sont des composés intéressants, utilisés dans divers procédés industriels. Toutefois, la grande stabilité thermodynamique et cinétique du CO_2 est la difficulté principale dans cette méthode. La conception d'un catalyseur capable de convertir le CO_2 de manière efficace est donc d'une importance fondamentale. Parmi les différents catalyseurs existants, les liquides ioniques à base d'imidazolium sont apparus comme d'excellents candidats.

Cette thèse de master en chimie est focalisée sur la synthèse de catalyseurs hétérogènes à base de nanocornes de carbone, fonctionnalisées avec des groupements imidazolium, nécessaires pour surmonter la stabilité du CO_2 et faciliter sa conversion en carbonates cycliques.

Mémoire de Master en Sciences Chimiques (Orientation Chimie du Vivant et des Nanomatériaux)

Finalité Approfondie

Janvier 2019

Promoteur : Prof. Carmela APRILE
Superviseurs : Carla CALABRESE, Esther CARBONELL-LLOPIS

UNIVERSITY OF NAMUR
School of Sciences
Secretariat of the Department of Chemistry
Rue de Bruxelles 61 – 5000 NAMUR
Phone : +32(0)81 72.54.44 – Fax : +32(0)81 72.54.40
E-mail : enseignement.chimie@unamur.be - www.unamur.be/sciences

Single Walled Carbon Nanohorns- and Single Walled Carbon Nanotubes-Based Catalysts for the Conversion of Carbon Dioxide

Alexey Ryabov

Abstract

Nowadays, the main source of energy comes from fossil fuels. One of the by-products in the combustion process is carbon dioxide (CO_2). In recent years, the development of new processes based on CO_2 conversion is receiving a lot of attention. The reason is a possible conversion of a waste into converting an abundant, renewable and readily available reagent into useful products.

Cyclic carbonates, synthesized by the reaction of carbon dioxide and epoxides, are interesting compounds used in various industrial processes. However, the main difficulty of this method consists in good thermodynamic and kinetic stabilities of CO_2. The design of a catalyst capable of an efficient conversion of CO_2 is therefore of fundamental importance. Among various existing catalysts imidazolium-based ionic liquids have emerged as excellent candidates.

This master thesis in chemistry is focused on the synthesis of heterogeneous catalysts based on carbon nanohorns, functionalized with imidazolium moieties, needed to overcome the stability of CO_2 and facilitate its conversion into cyclic carbonates.

Master thesis in Chemical Sciences (Orientation Chemistry of Life and Nanomaterials)

Research Focus

January 2019

Promoter : Prof. Carmela APRILE
Supervisors : Carla CALABRESE, ESTHER CARBONELL-LLOPIS

Acknowledgments

I would like to thank in first place my supervisor, Professor Carmela Aprile, not only for allowing me to make my master thesis in her laboratory, but also for her professionalism, patience, kindness, advices and comprehension during those years of thesis.

Also, I would like to thank my daily supervisors Carla Calabrese and Esther Carbonell Llopis for sharing with me their laboratory experience, their guidance and help during my laboratory experiments and writings and corrections of diverse documents during this master thesis.

I also would like to address special thanks for Adrien Comès, Alvise Vivian, Luca Fusaro and Lucia Bivona as their knowledge and advices had enlightened several parts in my work and helped in the advancement of the master thesis. Also, an acknowledgment goes to Alexandra Yeromina for her precious advices during the final period of writing.

I would like to mention my friends Alexey and Alexandre who were there in some difficult moments of this master thesis. You always had a positive impact on my moral either inside or outside of a student career. You were always there when I needed you the most. Thank you guys!

Some special acknowledgment goes to my parents: they were of a great help and of an outstanding support during my student career.

Once more, thanks to everyone who participated, from near or far, to the elaboration of this master thesis. All of you guys are awesome and I wish you good fortune in the upcoming projects. Cheers!

Table of Contents

I. ABBREVIATIONS

BET - Brunauer–Emmett–Teller;

BJH – Barret-Joyner-Halenda;

BV-Imi Br – 1,1'-[1,4-phenylenebis(methylene)]bis(3-vinyl-1H-imidazol-3-ium) bromide;

CCS – Carbon dioxide capture and storage techniques;

CNHs – Carbon Nanohorns;

CNTs – Carbon Nanotubes;

CO_2 – Carbon Dioxide;

ECH – Epichlorohydrin;

o-DCB – *ortho*-Dichlorobenzene

GHGs – Greenhouse Gases;

^{1}H-NMR – Proton Nuclear Magnetic Resonance;

Hz – Hertz;

ILs – Ionic Liquids;

IUPAC – International Union of Pure and Applied Chemistry;

MRI - Magnetic Resonance Imaging;

PSD – Pore Size Distribution;

SO – Styrene Oxide;

SSA – Specific Surface Area;

SWCNHs – Single Walled Carbon Nanohorns;

SWCNTs – Single Walled Carbon Nanotubes;

Bin-Mim-SWCNHs Br – Bingel modified Single Walled Carbon Nanohorns with 1-Methylimidazolium Bromide;

TEM – Transmission Electron Microscopy;

TGA – Thermogravimetric Analysis;

TON – Turnover Number;

II. INTRODUCTION

2.1. Carbon Dioxide: Environmental Impact and Solutions

Carbon dioxide is a small molecule made up of two atoms of oxygen bonded covalently to an atom of carbon (**Figure 2.1**). This gas has a huge environmental impact and is very important for the suitable for mankind life on Earth, as CO_2 is one of the greenhouse gases [1]. Those gases are responsible for the greenhouse effect [2]. Without GHGs, the average Earth temperature would be around -18 °C, instead of current 15 °C [3,4], making life on Earth quite difficult.

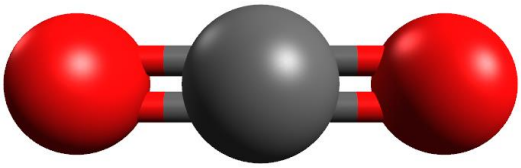

Figure 2.1 : Representation of a single CO_2 molecule; the grey sphere represents a carbon atom, and the red spheres represent oxygen atoms (was drawn with Avogadro software)

On the other hand, the amount of GHGs is constantly increasing in the atmosphere from year to year [5]. This phenomenon, mostly due to anthropogenic sources, causes climate changes that result in global warming, *i.e.* an increasing of the average Earth temperature. The scientific and industrial communities had to take a challenge on the reduction of dumping quantities of GHGs into the atmosphere in order to avoid potential noxious scenarios for Earth's biosphere [6].

Carbon dioxide capture and storage techniques were developed to reduce emissions of the concerned gas. Several strategies were already discussed in literature [7,8]. However, it seems that CCS might also have an important cost in terms of energy and may also have an important impact on the biosphere. Furthermore, CCS do require important financial investments that could lead to an important economic impact on our society [9,10].

While CCS are highly demanding in terms of energy and may introduce additional costs, recycling of CO_2 may represent an economically interesting and environmental friendly option.

Since CO_2 is an abundant, renewable and relatively cheap source of carbon, its conversion into useful chemicals represents a way to transform a waste into valuable products such as urea, formic acid, polycarbonates and cyclic carbonates [11–13]. For instance, cyclic carbonates are reported to be useful in various chemical reactions [14–16], as polar aprotic solvents [17], as well as in lithium ion batteries [18,19]. The last example is especially interesting due to constantly increasing market of fully electric and hybrid cars during last decade [20,21].

2.2. Catalysis

A catalyst is a species which allows lowering the activation energy of a chemical reaction thus increasing the rate of the process (**Figure 2.2**) [22]. Moreover, the catalyst should remain unchanged at the end of the reaction despite its interaction with reactants and products.

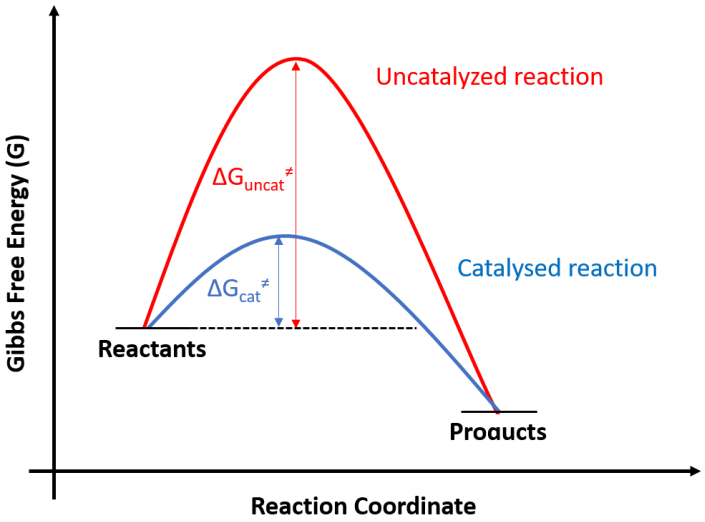

Figure 2.2 : Schematic representation of Gibbs free energy for the advancement of a chemical reaction; $\Delta G_{uncat}^{\neq}$ and $\Delta G_{cat}^{\neq}$ represent the variation of the Gibbs free energy for the activation of uncatalyzed and catalysed reactions respectively [22]

The choice of appropriate catalyst for a chemical reaction is especially important when working with industrial quantities of chemical compounds. A good catalyst for a reaction of interest is considered to have high activity and selectivity, long life time, to be nontoxic and cheap, as well as to be easily purified/regenerated after being used as many times as possible. [23]

2.3. Types of Catalysis

There are two global classes of catalysis: homogeneous and heterogeneous. For the homogeneous catalysis, the transformation of reactants into products, in presence of a catalyst, takes place in the same phase. In case of heterogeneous catalysis, the phases of reactants are different from the phase of a catalyst, generally a solid.

Each type of catalysis has its own advantages and disadvantages. For instance, in homogeneous catalysis, good dispersion of a catalyst in a reaction media results in high conversion and selectivity. Unfortunately, catalysts in the same phase as reactants and products are difficult to recover and to reuse. Also, products do have a higher risk of contamination by the catalyst when both are in the same phase. [23,24]

The problems related to contamination and recovery are largely reduced when using a heterogeneous catalyst which is present in a different phase from the reaction media (reactants, products, solvent). As a counterbalance, the activity of a heterogeneous catalysts is lower, if compared with its homogeneous analogous, thus resulting in lower yield. Despite this fact, heterogeneous catalysis is preferred by the industrial sector mostly for its easy separation from the reaction media [23,24]. However, the activity of a heterogeneous catalysts is influences by a large amount of different parameters such as surface area, pore size distribution, average particle dimension and shape, dispersion and accessibility of active sites, hydrophilic/hydrophobic balance of the catalyst surface among others, which are playing often a synergic role.

Nowadays, a lot of research activities are initiated on academic or industrial level in order to have a better understanding of the influence of all these parameters on the catalyst performances. By improving scientific knowledge, for instance in heterogeneous catalysis, it might be possible to obtain an easily recoverable catalyst with the advantages of its homogeneous analogous. Also, the improvement of catalytic activity in the reaction of interest may result in lower energy input, thus reducing costs while increasing or at least maintaining the overall catalytic performances.

2.4. Ionic Liquids and the Conversion of Carbon Dioxide

Ionic liquids (ILs) are defined as salts that can be liquid at temperatures lower than 100 °C. Those compounds are already known for a long time, but in recent years they are attracting growing interest of the scientific community from both scientific and industrial parties [25,26]. The reason of such interest is mainly related to the fact that ILs have a potential of becoming a widely used green solvents due to their low melting point, very low vapour pressure, thus low volatility, high thermal stability, and low toxicity. Moreover, there is a huge amount of possible combinations of anions and cations needed for a preparation of IL that can lead to the preparation of various ILs, thus allowing the modulation of properties of ILs for various chemical reactions [25–27]. As an example, some of the most used cations and anions are represented in **Table 2.1** [28].

Table 2.1 : Representation of some of the most used cations and anions for the ILs [28]

Cations			
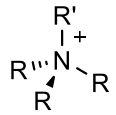	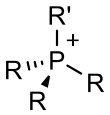	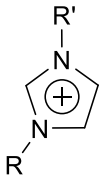	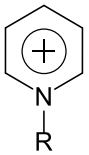
Tetraalkyl-ammonium	Tetraalkyl-phosphonium	*N,N'*-dialkylimidazolium	*N*-alkylpyridinium
Anions			
Cl^- Br^- I^-	BF_4^-	PF_6^-	$CF_3SO_3^-$	$N(CF_3SO_2)^-$
Halides	Tetrafluoroborate	Hexafluoro-phosphate	Trifluoro-methanesulfonate	Bis(trifluoro-methylsulfonyl)imide

Ionic liquids and in particular ammonium and imidazolium-based salts, displayed an excellent activity as homogeneous catalysts in the formation of cyclic carbonates from carbon dioxide and a large variety of epoxides[29–32]. The growing scientific and industrial interests for the synthesis of cyclic carbonates in ILs comes from a fact that it is a one pot reaction with a 100% atom economy and can be performed also under solvent free conditions. Indeed, in

most cases ILs play the role of a solvent and a catalyst at the same time, thus providing a low cost of the process. It deserves to be mentioned that CO_2 has a good solubility in ILs that can be further improved by using high pressure and temperature [28].

The mechanism describing the synthesis of cyclic carbonates from an epoxide and CO_2 in presence of an imidazolium-based catalyst is shown in **Scheme 2.1**. This pathway is largely described in literature [15,33,34].

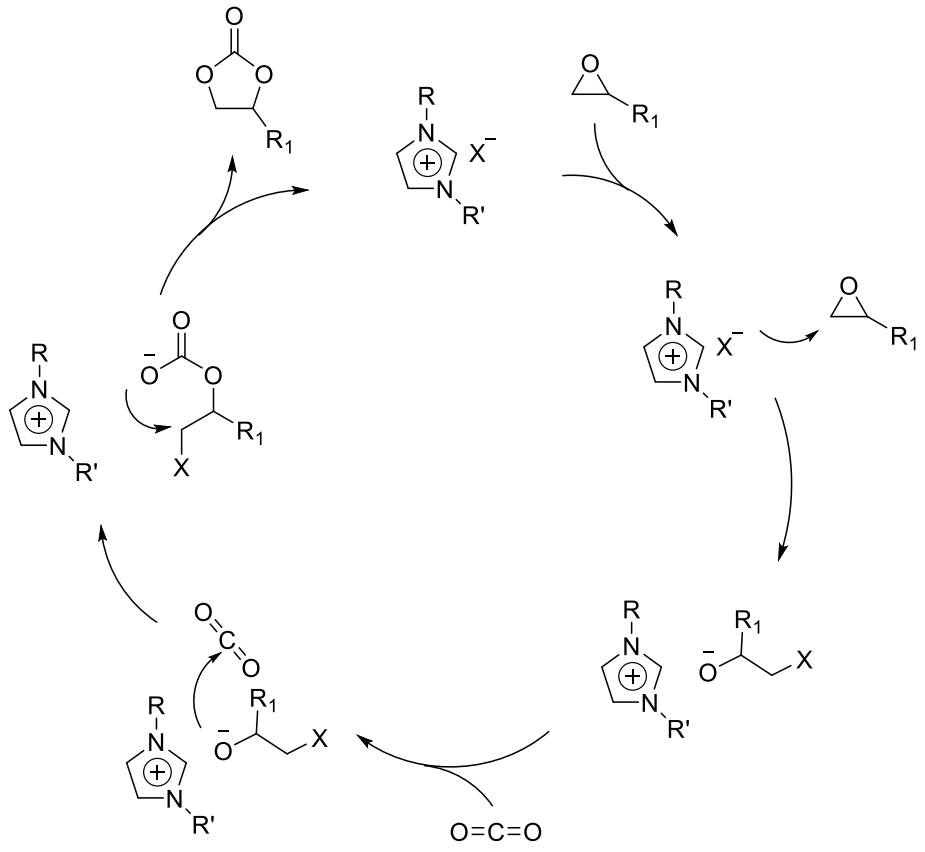

Scheme 2.1 : Proposed mechanism for the synthesis of cyclic carbonates via reaction of CO_2 with monosubstituted epoxides catalysed by supported imidazolium-based salts; X^- is counterion of *N,N'*-dialkylimidazolium and acts as a nucleophile [15,33,34]

In present example, the reaction starts with the nucleophilic attack of X^- (a counter ion of *N,N'*-dialkylimidazolium) to the epoxide. The strained ring opening generates an alkoxide which in turn attacks the electrophilic carbon of CO_2. The last step is an intramolecular nucleophilic substitution where X^- acts as a leaving group, thus regenerating IL and forming a cyclic carbonate.

2.5. Heterogenized Catalyst

Traditionally, the fields of homogeneous and heterogeneous catalysis are considered as two distinct domains. However, there are various ways in which a homogeneous catalyst can be converted in a heterogeneous one via functionalization of an appropriate support. This last approach is usually known as "heterogenization" A heterogenized catalyst is a combination of two parts, generally attached to each other directly through a covalent bond or *via* a linker, where one part is a homogeneous catalyst and the other one is a solid support/a catalytic support (**Figure 2.3**). [35]

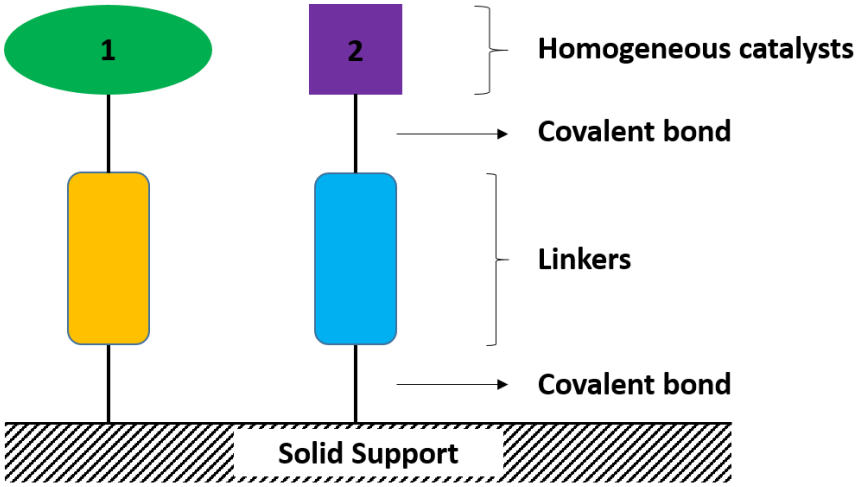

Figure 2.3 : Schematic representation of two different homogeneous catalysts heterogenized on the surface of a solid support/catalytic support with two different linkers

The main reason for a heterogenization process of homogeneous catalysts is the easier recovery of the catalyst from the reaction media and the consequent possible reuse in multiple catalytic cycles. Furthermore, sometimes, depending on the support, the surface of the solid may also play an active role, acting as a co-catalyst. In this case, a new catalyst might appear to be even more efficient than its homogeneous analogous. Another positive point is the possibility to graft two or more homogeneous catalysts on solid support, leading to one pot multi-stage reactions without need in recovery of intermediate products. [35]

It is important to mention that several issues should be taken into an account for the heterogenization process of homogeneous catalysts. For instance, a homogeneous catalyst might need a chemical modification resulting in a binding group that is required for its covalent attachment on the surface of a catalytic support or to a linker. This modification can provoke changes in the activity and/or selectivity of a catalyst. Also, a passage from homogeneous catalyst to heterogenized one changes the dispersion of the catalyst in the reaction media, thus again having an impact on the catalytic activity, and making reaction slower compared to homogenous analogous. Nevertheless, the fact that the catalyst is in a different phase than the reactants and products facilitates its separation and recovery from the reaction media. Even though the speed of reaction with heterogenized catalysts is often reduced, whole reaction process is performed faster since separation and recovery of the catalyst as well as of the reaction products are performed faster. [35]

2.6. Catalytic supports

2.6.1. Single Walled Carbon Nanohorns

As discussed previously, the support plays an important role in heterogenization process and it will strongly influence the catalytic performances of the final catalyst. Several parameters should be taken into account for the correct choice of the solid support such as toxicity, thermal stability, surface area and pore size distribution [35]. In particular, carbon-based nanomaterials such as polymers, carbon nanotubes and carbon nanohorns are often reported in literature as suitable supports for the heterogenization of ILs for the design of hybrid catalyst able to promote the reaction between CO_2 and epoxides into cyclic carbonates [36–38].

For instance, single walled carbon nanohorns are one of synthetic forms of carbon allotropes. They were discovered by Iijima *et al.* in 1998 [39]. The synthesis of SWCNHs was initially achieved by CO_2 laser ablation of pure graphite without using metallic catalysts, thus achieving very high purities and a high yield compared to carbon nanotubes. SWCNHs are made of single-wall sp2 carbon sheet that have a horn-like conical structure closed at one end. The conical shape is given by a pentagonal ring, or an assembly of pentagonal rings, at the closed end of the cone. This structure is extended by hexagonal graphenic network thus forming a bigger conical structure – carbon nanocones [40]. The diameter of those cones varies approximatively from 2-5 nm for 40-50 nm in length. The conical tip, with an average opening angle around 20° makes carbon nanohorns similar to fullerenes and their elongated structure have a lot in common with carbon nanotubes (**Figure 2.4**, left) [41].

During the synthesis, individual nanocones aggregates into clusters and get covalently attached to each other [42] with the possibility of forming one of three known types of SWCNHs: bud-like, seed-like and dahlia flower-like carbon nanohorns [43]. The size of those aggregates varies between 50 nm and 150 nm, and strongly depends on the synthetic technique and experimental conditions used for the synthesis (**Figure 2.4**, middle and right) [41,43].

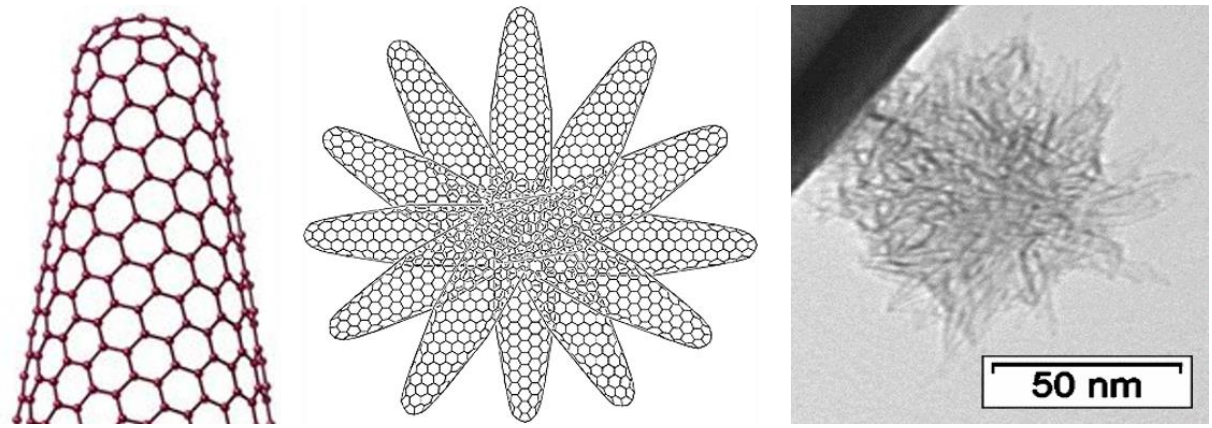

Figure 2.4 : Schematic representation of a single walled carbon nanocone/nanohorn (left) and agglomerated dahlia flower-like structure of carbon nanohorns(centre, adapted from [44]**)**, as well as an actual TEM picture of a dahlia-like structure of aggregated nanocones (right)

CNHs can be obtained *via* arc discharge, laser ablation or Joule heating. All methods require an important amount of energy and don't use any metallic particles for the synthesis of carbon nanostructures. The amount of produced CNHs may vary from one to several kilograms per day, depending on the method and experimental conditions, with fairly high product purity ranging from 85 % to 95 %, with no post-synthetic purification step required in most cases. [41]

Although CNHs are a relatively new material, it already has several potential applications. The interest directed in the favour of this particular form of carbon allotrope is due to its clean structure, with only a small quantity of amorphous carbon, and a total absence of metallic contaminants. For instance, carbon nanohorns could be as a gas storage material where they have shown some good results. CNHs could also be potentially used as a drug carrier since it has a low toxicity on the human body. Due to its particular properties, CNHs may also be used as biosensors, electrodes, catalytic supports, gas sensors, photovoltaics, as a support for contrast products during MRI scans, etc. [41,43,45].

2.6.2. Single Walled Carbon Nanotubes

Single walled carbon nanotubes are another synthetic carbon allotrope (**Figure 2.5**). They were discovered by Iijima in 1991 [46] and reported in 1993 [47]. There are several possible procedures that lead to the synthesis of carbon nanotubes. The most used are electric arc deposition, arc discharge method, and chemical vapour deposition. The purification step comes after the synthesis, where nanotubes are treated in acid solutions for their purification: removal of large graphite particles and catalysts [48,49].

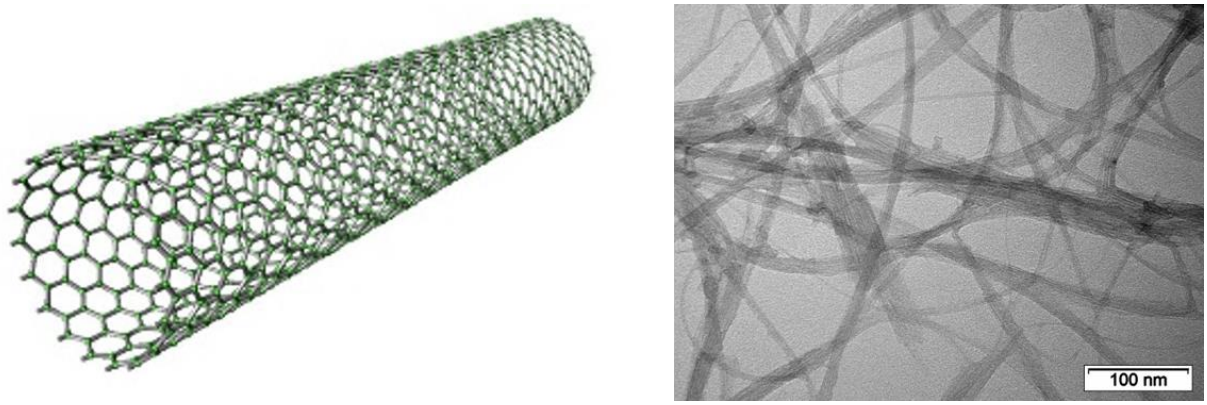

Figure 2.5 : Schematic representation of single walled carbon nanotube (left) and image of SWCNTs bundles observed with TEM

Single walled carbon nanohorns present themselves as a rolled up sheet of graphene, thus made of sp2 carbon atoms, into a tube of 1,2 – 1,4 nm in diameter, and about a micrometre long [48]. Its surface area is approximatively 1600 m^2/g. CNTs also have pores with average size around 4,0 nm [50].

Due to the properties of CNTs [51], a lot of ideas for their potential application had emerged [48,49], among which CNTs can be found as a reinforcement material and energy storage media [52,53], they can be used as composite materials and in electronics [53,54], in drug delivery [55], as well as a catalytic support [56].

III. OBJECTIVES

The main objective of this master thesis was the synthesis and characterization of novel imidazolium-based heterogeneous catalysts prepared *via* heterogenization of imidazolium salts covalently anchored to the surface of SWCNHs. The idea was to have a catalyst which may bridge the gap between homogeneous and heterogenous systems, hence able to efficiently promote the conversion of carbon dioxide and monosubstituted epoxides into cyclic carbonates (**Scheme 3.1**).

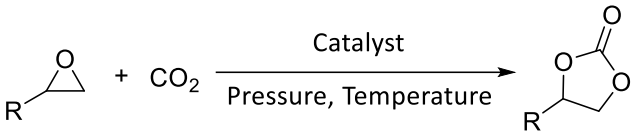

Scheme 3.1 : Synthesis of cyclic carbonates from monosubstituted epoxides and CO_2

Three synthetic routes were initially planned for the grafting of imidazolium salts onto the surface of CNHs: an oxidation of SWCNHs followed by esterification, a Bingel cyclopropanation and a radical polymerization. These synthesis approaches were compared employing several criteria such as time of the synthesis, control and reproducibility of the functionalization and amount of functionalization. In some case, catalytic activity in terms of leaching, TON, reuse, etc. was also selected as parameter for the correct choice of the most promising catalyst.

The synthesis of cyclic carbonates from CO_2 and an epoxide catalysed by the upgraded catalyst was also performed under different reaction conditions.

IV. STRATEGIES

Since imidazolium-based salts showed themselves as very efficient homogeneous catalysts for the conversion of CO_2 and epoxides into cyclic carbonates, it does seem interesting to heterogenize these salts. As mentioned previously, the main advantage of this strategy would be an easy recovery of the heterogenized catalyst from the reaction media, and its reuse in consecutive cycles. [37,57,58]

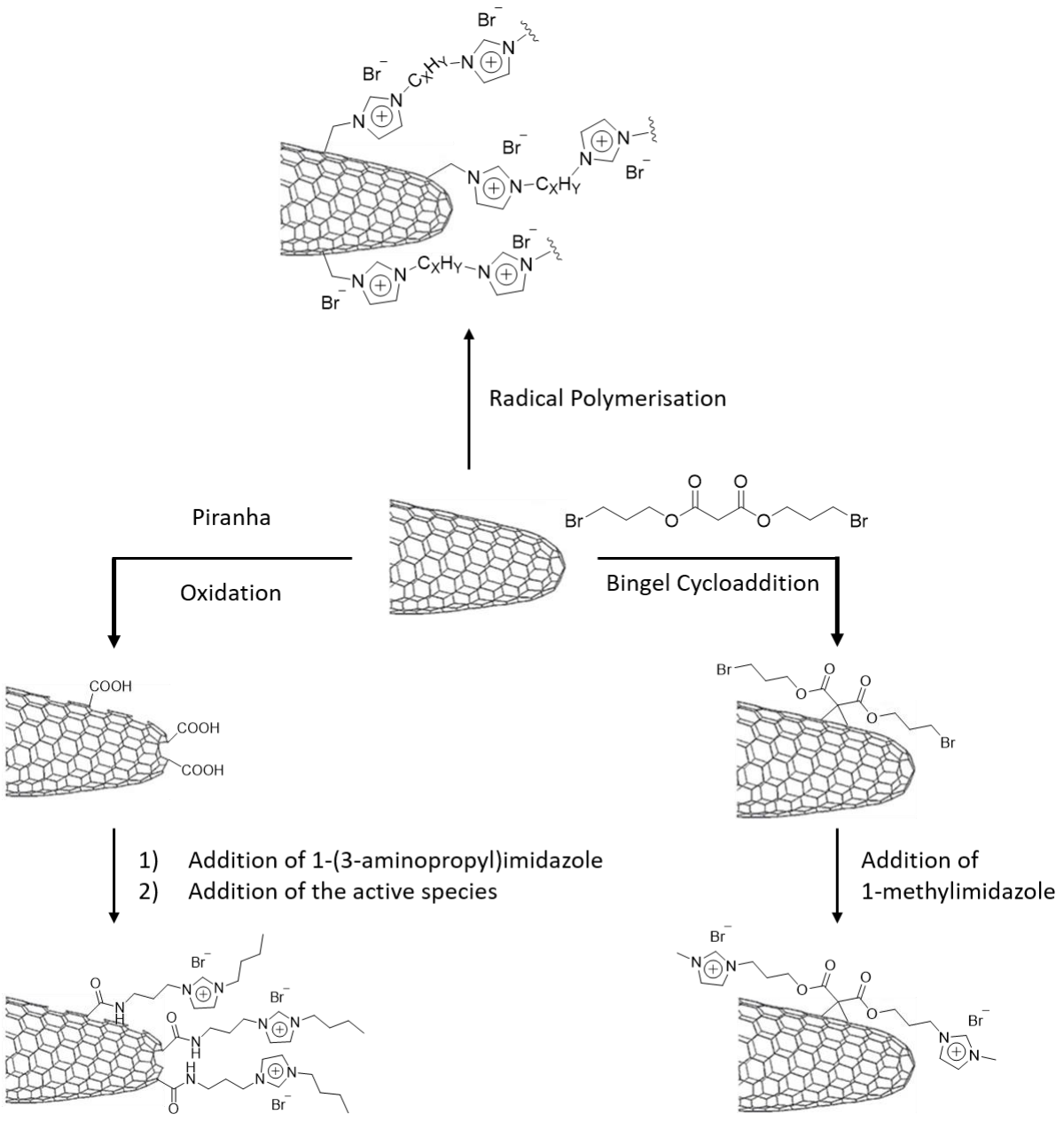

Scheme 4.1 : Schematic representation of three different methods used in this master thesis for the modification of the surface of pristine SWCNHs with imidazolium-based molecules

Herein, SWCNHs were selected as catalytic support owing to their interesting properties such as their chemical and mechanical stability combined with their high dispersibility in many organic solvents

SWCNHs had to be modified in three different ways (**Scheme 4.1**). All three modifications of nanohorns were adapted from literature, since they were already reported for other carbon allotrope: radical promoted polymerization of imidazolium-based salts [37], the oxidation of carbon nanostructures by piranha solution followed by modification of carboxylic moieties and further addition of active species [59,60], and modification of carbon nanostructures by Bingel cyclopropanation reaction [61]. Several molecules, such as BV-Imi Br and bis(3-bromopropyl) (**Scheme 4.2**) malonate were needed to be synthetized as they had served as the precursors of the active species in radical polymerisation and Bingel cyclopropanation respectively.

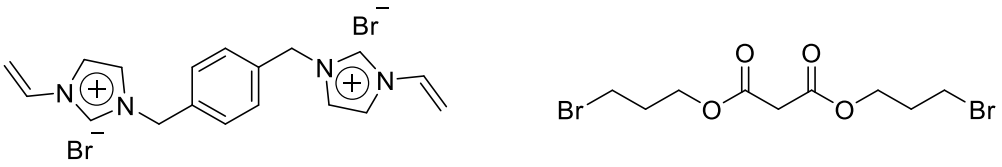

Scheme 4.2 : BV-Imi Br (left) and bis(3-bromopropyl) malonate (right)

After the synthesis, the materials were submitted for a series of analysis: TEM for the morphologic analysis of each material, TGA for the procuration of the quantity of the active species present in the material and N_2 adsorption/desorption for the surface area analysis. Each technique served to compare materials with their pristine analogous, as well as to compare synthetic products between themselves. As for the precursors of active species, their structure was verified by ^{1}H-NMR spectroscopy.

Next step of the master thesis was the verification of the catalytic activity for each material. Chemical reaction used for this purpose was the reaction between an epoxide and CO_2 in order to form a cyclic carbonate (**Scheme 4.3**).

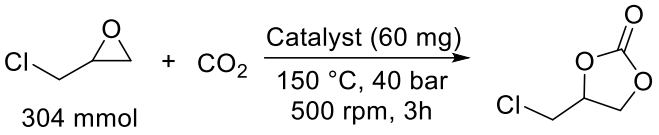

Scheme 4.3 : Reaction conditions used in this master thesis to test the catalytic activity of synthetized materials; Synthesis of 4-(chloromethyl)-1,3-dioxolan-2-one from epichlorohydrin and CO_2

Also, the imidazolium-functionalized materials had undergone a recycling test in order to put into perspective the activity, the longevity and the covalent attachment of active species to the surface of the catalyst. The experimental conditions are similar to the primary catalytic tests, except epichlorohydrin was replaced with styrene oxide, and twice the amount of a catalyst were used (**Scheme 4.4**).

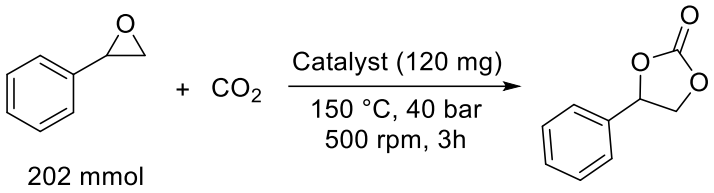

Scheme 4.4 : Reaction conditions used in this master thesis for the recycling tests of synthetized materials; Synthesis of 4-phenyl-1,3-dioxolan-2-one from styrene oxide and CO_2

In both cases, the conversion of epoxide into the corresponding cyclic carbonate was followed by ^{1}H-NMR spectroscopy. Knowing the proportion of epoxide to cyclic carbonate as well as the amount of active species that was present in the catalyst by TGA, it was possible to calculate TON. In case of this master thesis, TON may be written as in equation (**4.1**).

$$TON = \frac{Number\ of\ moles\ of\ an\ epoxide\ converted}{Number\ of\ moles\ of\ the\ active\ sites} \qquad (\mathbf{4.1})$$

In this master thesis, TON shows the amount of converted epoxide per mole of an active sites and allowed to compare different materials from different synthetic methods by their catalytic activity and determine the one with greater conversion, as well as it allows the comparison of materials obtained in this master thesis with those described in literature.

Another way to compare obtained materials is Productivity. In case of this master thesis, Productivity is calculated as it is showed in the equation (**4.2**).

$$Productivity = \frac{Mass\ of\ converted\ reactants}{Mass\ of\ a\ catalyst} \quad (\mathbf{4.2})$$

The synthesis method that led to the catalyst with the most important conversion of reactants into product had a deeper investigation in it. For this purpose, the reaction conditions of the chosen method were modified in order to optimise the heterogeneous catalyst and make it more efficient in the synthesis of cyclic carbonates.

The main idea of the optimised catalyst was to reduce the energy input in the synthesis of cyclic carbonate by a greater ratio than its precursors. For this purpose, this catalyst was used under different reaction conditions in the synthesis of cyclic carbonates, such as a lower temperature and a presence of a co-catalyst in the reaction medium.

V. RESULTS AND DISCUSSION

In this section are discussed the materials obtained by the different synthetic approaches described in the previous section, as well as their characterisation and catalytic results.

5.1. Oxidation of SWCNHs

The first approach selected in the master thesis, was the oxidation of SWCNHs surface with a piranha solution (22mL of H_2O_2 [30%] slowly added to 88 mL of H_2SO_4 [98%]), where 1 mL of piranha was used for the oxidation of 1 mg of CNHs. The oxidative treatment should generate carboxylic functionalities suitable for the post-functionalization with imidazolium active species (**Scheme 5.1**).

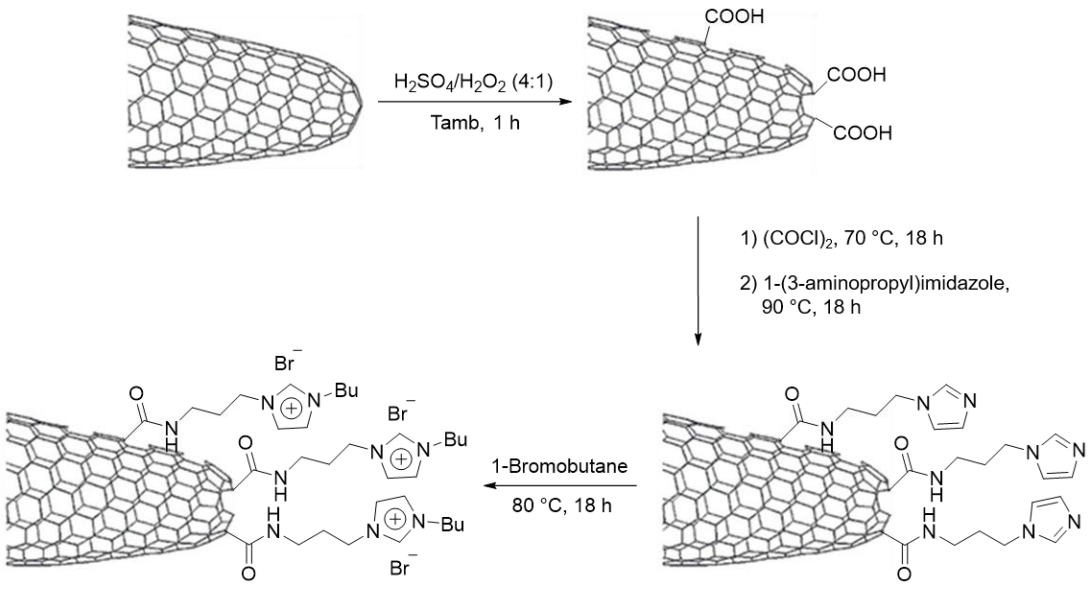

Scheme 5.1 : Representation of the synthesis of SWCNHs and imidazolium-based heterogeneous catalyst from initially oxidized carbon nanohorns by a piranha solution

However, the oxidative treatment appeared to be difficult to control. It was noticed that individual dahlia-like shape of the material, as well as their conical ends were no more detectable by TEM (**Figure 5.1)** after treatment. This observation was attributed to the collapse of the organised conical nanohorn structure [40]. Different attempts were performed with similar difficulties.

Since this oxidation process on SWCNHs did not achieve the expectations, as well as the experimental methods performed in parallel were showing promising results, this method was left without further investigations. Nevertheless, the alternative types of oxidation might be explored in future works [62,63].

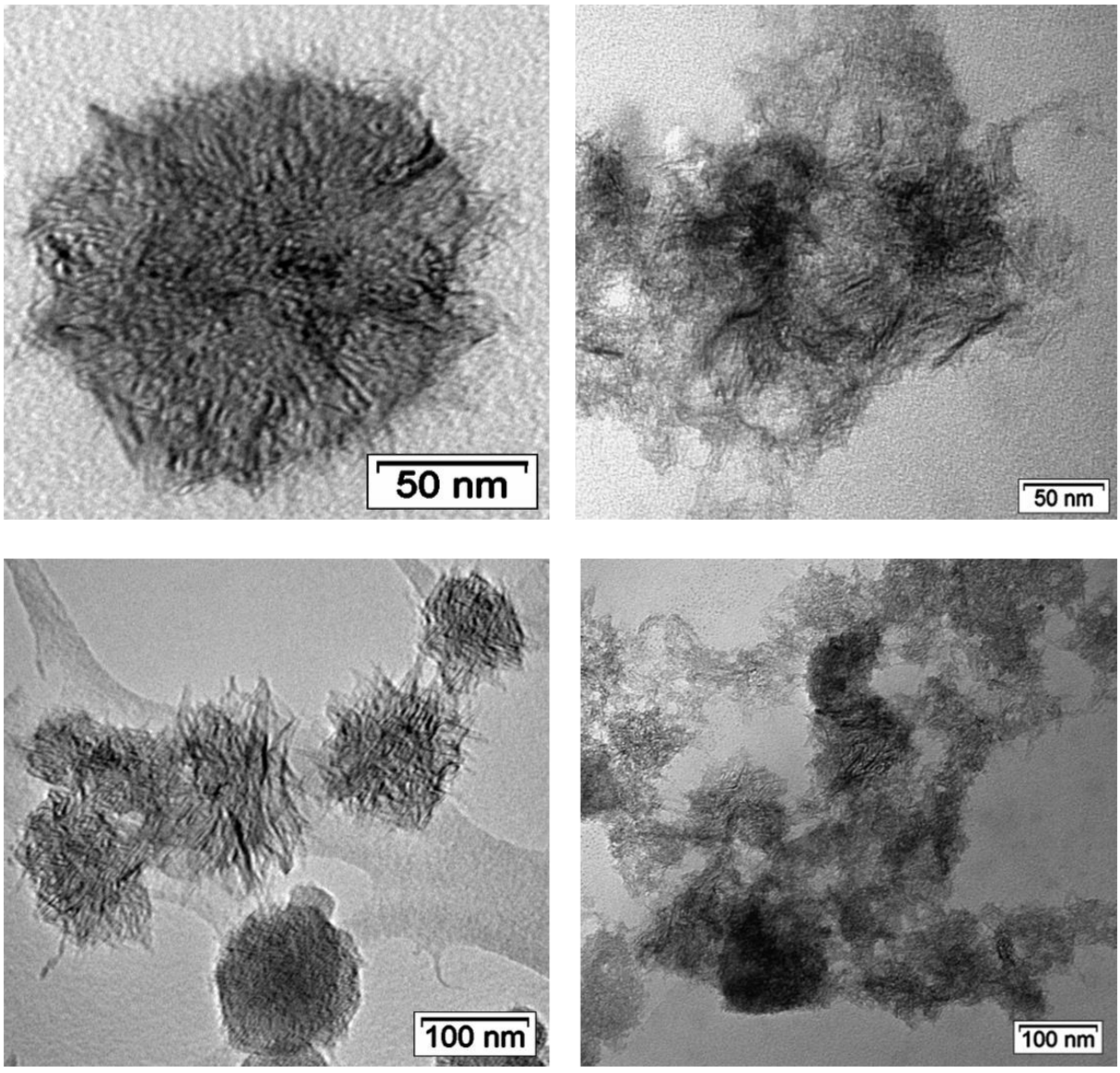

Figure 5.1 : SWCNHs pristine (left) and after the oxidative treatment (right); the dahlia-like structures cannot be found after the treatment of SWCNHs with piranha solution

5.2. Bingel Cyclopropanation on SWCNHs

The Bingel cyclopropanation reaction was another method employed to modify the surface of SWCNHs. This method was initially performed on the fullerenes [61,64], and later was extended to other carbon nanostructures, such as carbon nanotubes [65,66] and graphene [67,68]. There attempts to perform a "traditional" Bingel reaction on the surface of CNHs are also described in literature [69].

Bis-(3-bromopropyl) malonate, synthetized from the reaction between malonyl chloride and 3-bromo-1-propanol, reacted on the surface of SWCNHs *via* Bingel cyclopropanation reaction. Then, Bin-Mim-SWCNHs Br was synthetized by adding to 1-methylimidazole to the structure of the previous product. The final material was characterized *via* various technique including TEM (**Figure 5.2**) and TGA (**Figure 5.3**).

The TGA showed that there was a difference in thermogravimetric curves between pristine SWCNHs and functionalized material. Pristine nanohorns are relatively stable up to 800 °C, whereas the materials after of each step of functionalization showed a mass loss due to the presence of bis(3-bromopropyl) malonate and its 1-methylimidazolium analogue. The difference between TGA curves were made at 600 °C. The difference functionalized materials is equal to a weight loss of 2,50 %. Knowing this difference, and knowing the molar mass of 1-methylimidazole (82,10 g.mol^{-1}), it was possible to estimate the loading of the active species present on the catalytic support *via* equation (**5.1**).

$$n = \frac{m}{M_M} = \frac{25{,}0.10^{-3}}{82{,}10} = 0{,}3.10^{-3}\ \text{mol}.g^{-1} \qquad (\mathbf{5.1})$$

Where: n (mol.g^{-1}) – number of moles of catalytic species per gram of heterogeneous catalyst;

m (g) – the loading of the catalytic support with the active species;

M_M (g.mol^{-1}) – molar mass of 1-methylimidazole.

TEM didn't show any visible differences between pristine and functionalized materials most likely due to a fairly small size of the attached molecule, and/or the insufficient resolution of the electronic microscope, assuming that the synthesis of the catalyst was achieved well.

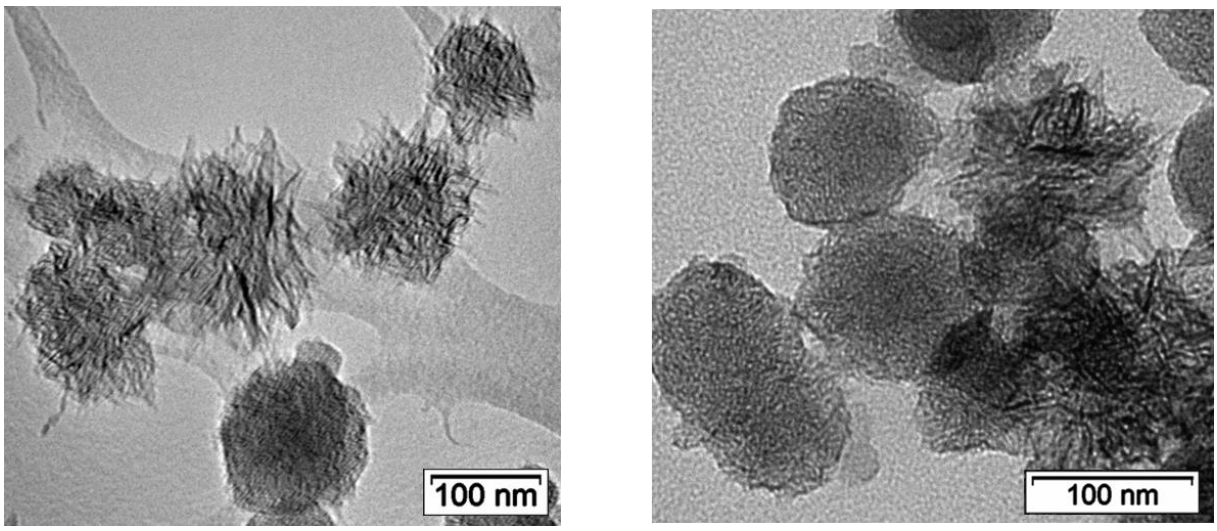

Figure 5.2 : TEM of pristine SWCNHs (left) and their analogous after Bingel cyclopropanation reaction (right)

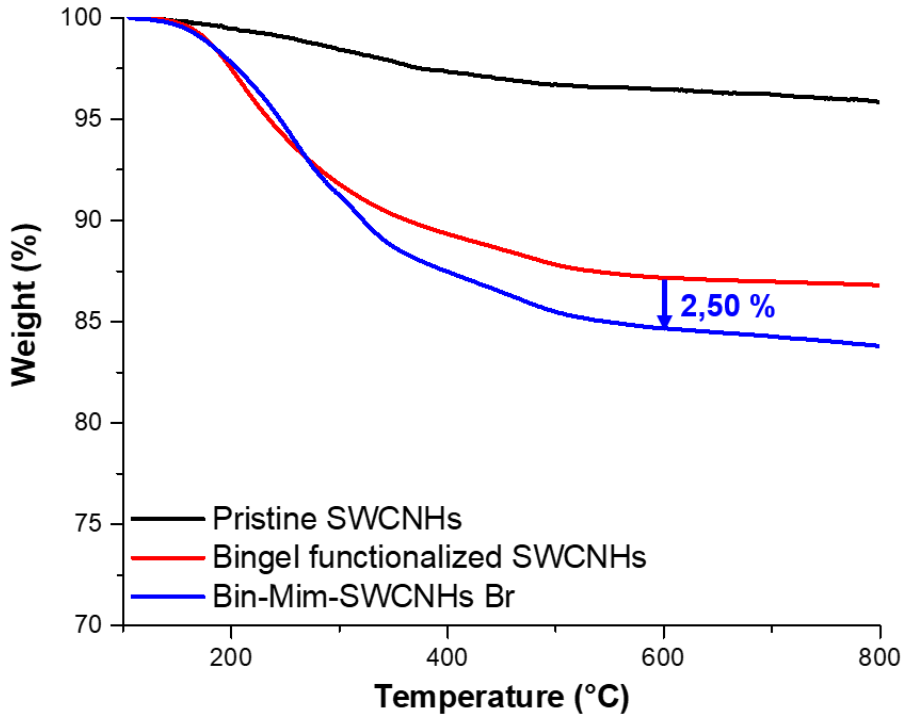

Figure 5.3 : TGA of pristine SWCNHs, its modification with bis(3-bromopropyl) malonate (red), and the attachment of 1-methylimidazole on bis(3-bromopropyl) malonate (bin-mim-SWCNHs Br, blue)

TGA analysis was used to quantify the amount of organic functionalization. In agreement with the previously reported literature data [69], a low degree of covalent functionalization (9,30 %) was observed on the surface of CNHs after the reaction. This result was attributed to the lower reactivity of SWCNHs compared to fullerenes as well as to the fact that the functionalization is performed under heterogeneous conditions (since SWCNHs are insoluble in the reaction medium). Hence, the reaction conditions were slightly changed in order to counterbalance the insolubility of CNHs and increase the percentage of functionalization. After optimization, the preparation of SWCNHs bearing a 2,50 % of imidazolium functionalization was achieved through Bingel reaction followed by nucleophilic substitution with 1-methylimidazole.

5.3. Heterogenization of BV-Imi Br

5.3.1. First Method

The third synthetic strategy for the preparation of the carbon nanohorns-based catalysts involves the use of the radical polymerisation approach. This method was already described in literature for the functionalization of silica based structured solids [37] and it was recently extended to SWCNHs. For comparison, the same approach was also applied to single walled carbon nanotubes. Two batches for both studied carbon allotropes were prepared: **T1**, **H1** and **T2**, **H2**, where **T** and **H** stand for SWCNTs and SWCNHs respectively, and **1** and **2** denote the amount of BV-Imi Br used for the synthesis of novel materials – 1,06 mmol and 2,13 mmol respectively. All synthetized materials were characterized *via* a series of experimental techniques, such as TEM, TGA, N_2 adsorption/desorption.

TEM investigation revealed the different morphology of the support used as well as their modification as function of the imidazolium loading. In case of SWCNTs (**Figure 5**), the pristine nanomaterials (**Figure 5 A, B**) are seen as the tick grey lines. The presence of various bundles as consequence of the $\pi-\pi$ staking interaction between the nanotubes wall can be clearly distinguished in the picture. On these images, the carbon nanotubes are clearly seen without any visual obstructions.

In case of the **T1** material (**Figure 10 C, D**), the striking difference compared to the pristine materials can be clearly seen. The nanotube bundles are covered with a polymeric network of BV-Imi Br. This network is distributed inhomogeneously over the surface of all pristine SWCNTs: the clear regions suggest that the polymeric network is either absent, or simply not thick enough to be observed by TEM. The darkest regions indicate the presence of thicker layers of polymeric network.

Despite the initial difference in BV-Imi Br loadings, **T2** material (**Figure 10 E, F**) does not display strong morphologic differences from **T1**. A similar polymeric network can be seen covering carbon nanotubes bundles inhomogeneously. Under a lower magnification, the

inhomogeneous distribution of BV-Imi Br polymer is even more noticeable, as it forms a sort of islets over the nanomaterial.

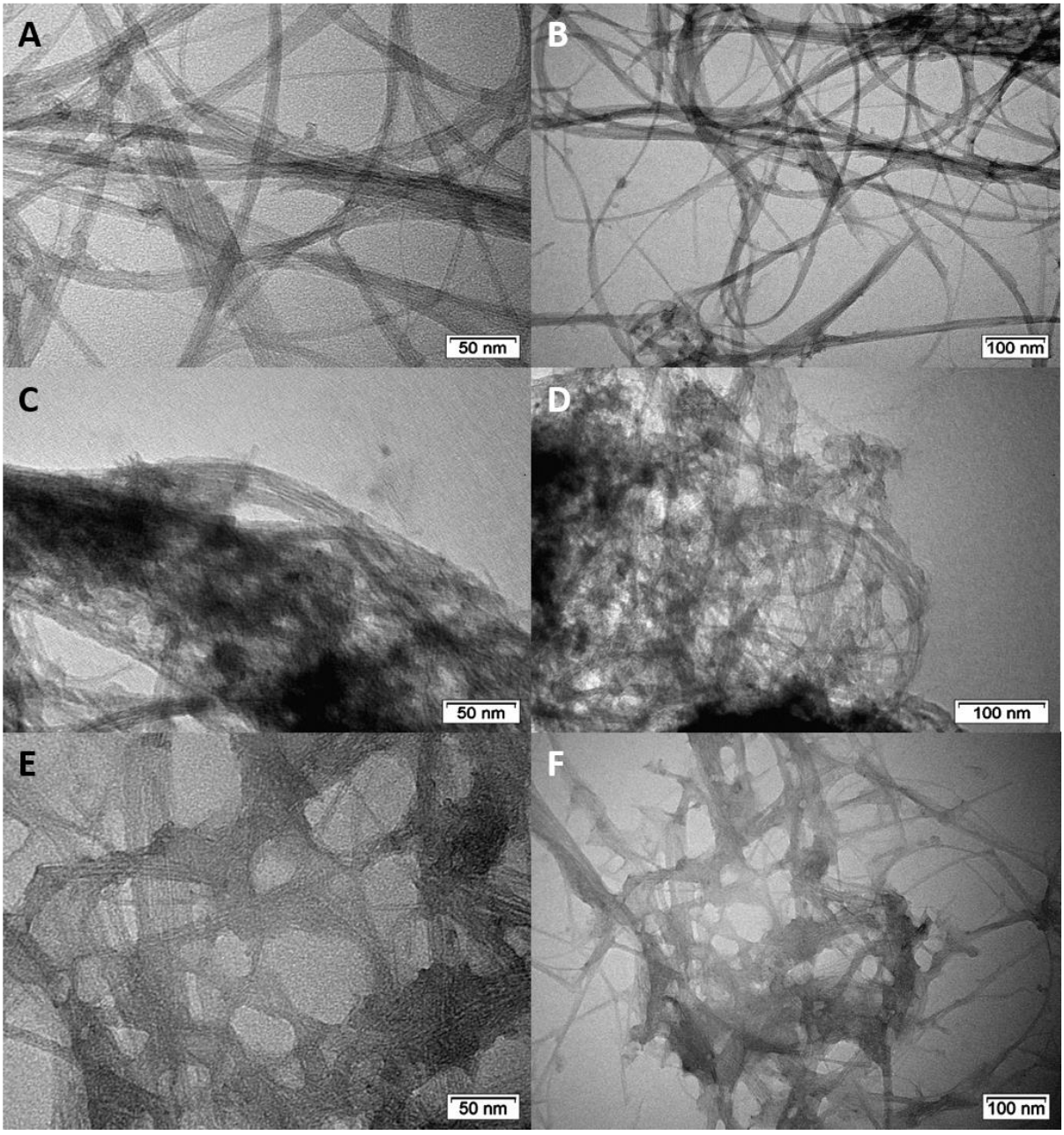

Figure 5.4 : TEM of SWCNTs-based materials under different magnification: A, B – pristine, C, D – **T1** material, and E, F – **T2** material

Pristine SWCNTs (**Figure 11 A, B**) also differs from its **H1** (**Figure 11 C** and **D**) and **H2** (**Figure 11 E** and **F**) analogous. After the polymerization reaction carbon nanohorns seem to be covered by a dark shell which was attributed to the presence of BV-Imi Br. The individual

dahlia-like nanohorns can be still be distinguished in the internal part of various nanostructures. Moreover, a morphological difference between **H1** and **H2** materials was clearly observed: the polymeric shell surrounding **H1** material was barely visible, whilst the shell of the same polymer around **H2** solids was more evident. This is most likely due to the amount of BV-Imi Br initially present for the synthesis of both materials: a higher amount of BV-Imi Br in the synthesis mixture produced a ticker polymeric shell.

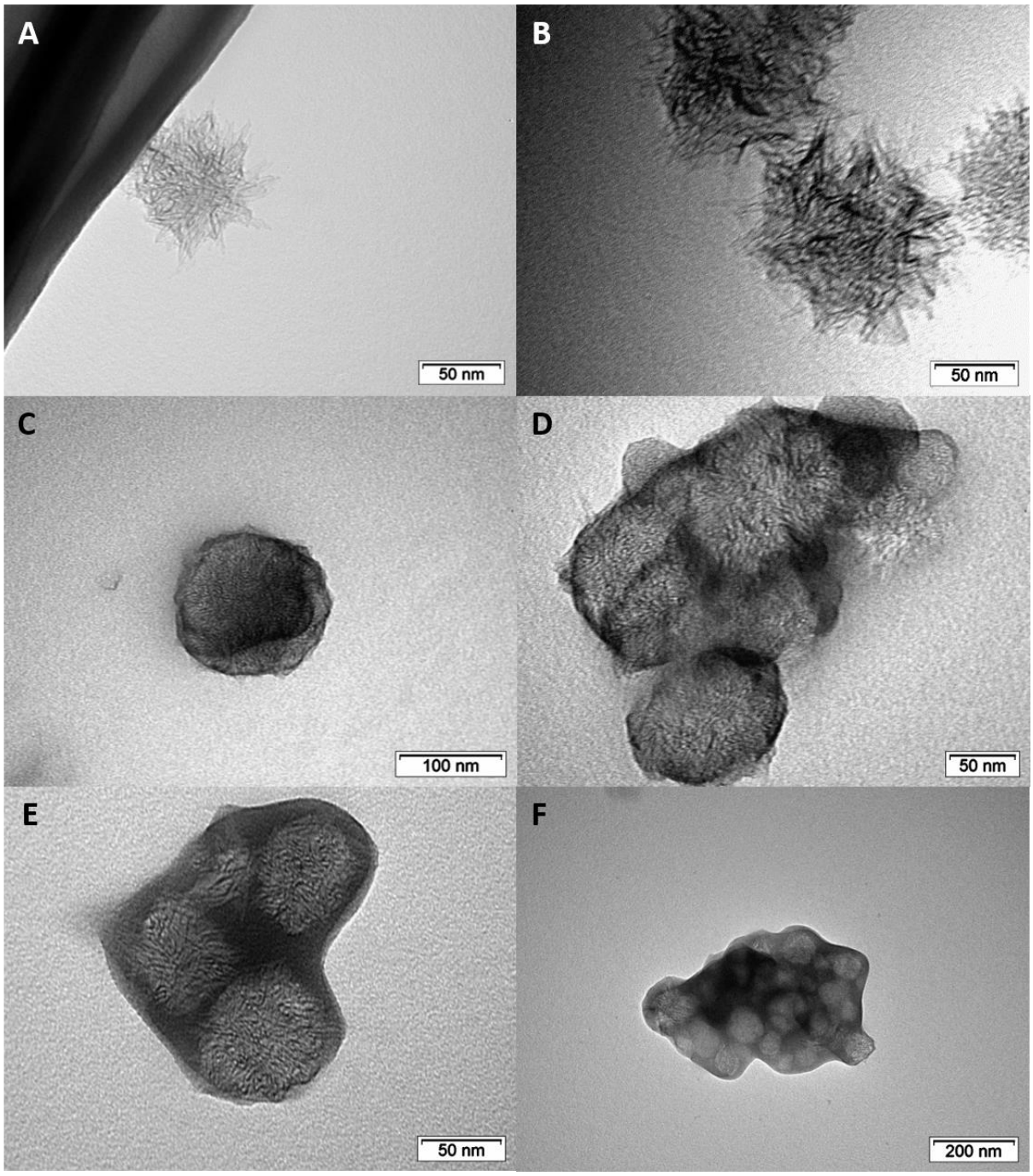

Figure 5.5 : TEM of SWCNHs-based materials under different magnification: A, B – pristine, C, D – **H1** material, and E, F – **H2** material

Table 5.1 summarizes the important values for both experiments performed on SWCNHs and SWCNTs. The observed tendency is that if the amount of BV-Imi Br is doubled, the amount of material recovered after the synthesis doubles as well.

Table 5.1 : The initial amount of SWCNTs and SWCNHs and BV-Imi Br used for the synthesis of heterogeneous catalysts, and the amount of recovered materials after the reaction; **H** and **T** stand for nanohorns and nanotubes respectively

Synthesis	**Amount of Carbon Nanomaterials** (mg)	**Initial BV-Imi Br Loading** (mmol)	**Recovered Material** (mg)
T1	130	1,06	195
T2	130	2,13	412
H1	130	1,06	177
H2	130	2,13	344

TGA was the second characterization technique applied to new materials in order to estimate quantitatively the amount of the BV-Imi Br attached to the surface of carbon nanostructures (**Figure 5.6**), and consequently the amount of active species – the bromide.

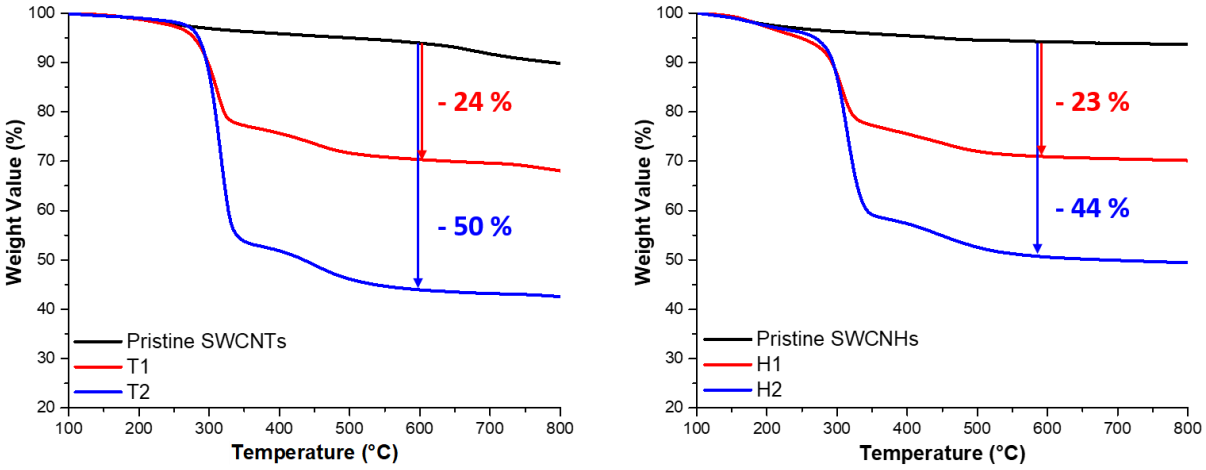

Figure 5.6 : TGA of pristine SWCNTs with **T1** and **T2** materials (left), and TGA of pristine SWCNHs with **H1** and **H2** materials; **T** stands for carbon nanotubes and **H** for carbon nanohorns

The thermogravigrams start at 100 °C and end at 800 °C. Beyond 800 °C, the structural integrity either of pristine, or of functionalized materials is lost. It is important to notice that

pristine SWCNHs seem to be more stable thermally compared to pristine SWCNTs. The origin of this inequality is most likely located in the different nature of these nanostructured carbon materials.[70]

In order to estimate the amount of BV-Imi Br attached to the surface of each carbon nanostructure, the difference in the weight value between pristine and functionalized materials should be converted in the number of moles of BV-Imi Br. This difference was evaluated at 600 °C. Knowing the molar mass of BV-Imi Br (452,19 g.mol^{-1}), the estimation of loading was made through the equation (4):

$$n_{BV-Imi\ Br} = \frac{X}{100} * \frac{1}{452{,}19} \qquad (\mathbf{5.2})$$

where X (%) is extracted from the TGA curves and represents the weight loss percentage per 100 grams of material, and $n_{BV-Imi\ Br}$ (mmol.g^{-1}) is the number of millimoles of BV-Imi Br per gram of concerned material. As it was mentioned previously, the active species for the catalysis of cyclic carbonates from CO_2 and an epoxide are bromides, and there are two bromides per molecule of BV-Imi Br. The results of the calculations are summarized in **Table 5.2**, and will be used further to calculate TON.

Table 5.2 : The amount of BV-Imi Br and of Br^- on the surface of the carbon nanostructures, calculated with equation (**5.2**) from the weight loss values obtained by TGA; **H** and **T** stand for carbon nanohorns and carbon nanotubes respectively

	T1	**T2**	**H1**	**H2**
$\boldsymbol{n_{BV-Imi\ Br}}$ (mmol.g^{-1})	0,52	1,11	0,51	0,96
$\boldsymbol{n_{Br-}}$ (mmol.g^{-1})	1,04	2,21	1,03	1,93

The functionalization strategy, initially used for SWCNTs, allowed to fix only about 50 % of BV-Imi Br on the surface of each carbon nanostructure. The slight difference in loadings of each sample might come from dissimilarities in the structure and the morphology of studied carbon allotropes.

Last characterization technique used was N_2 adsorption/desorption. It allowed to estimate the specific surface area for each material and its variation with the polymerization of BV-Imi Br on the surface of each pristine carbon nanostructure. It is important to mention that the analysis of some materials had failed mostly for technical reasons, such as unavailability of a sufficient mass of needed material to perform the analysis. This was the case of pristine SWCNTs and **T1** material. Missing data for pristine materials was found in literature.

Pristine single walled carbon nanotubes has a specific surface area around 1000 m^2 per gram of material [37]. Their pore size distribution is generally lower than 2 nm in diameter and is attributed to the openings at both ends of a carbon nanotube. This ranges SWCNTs into microporous materials after the IUPAC classification [72], even though the presence of meso- and macro-pores is not excluded. The presence of meso- and macro-pores is due to the interstices between nanotubes when they aggregate into bundles [73].

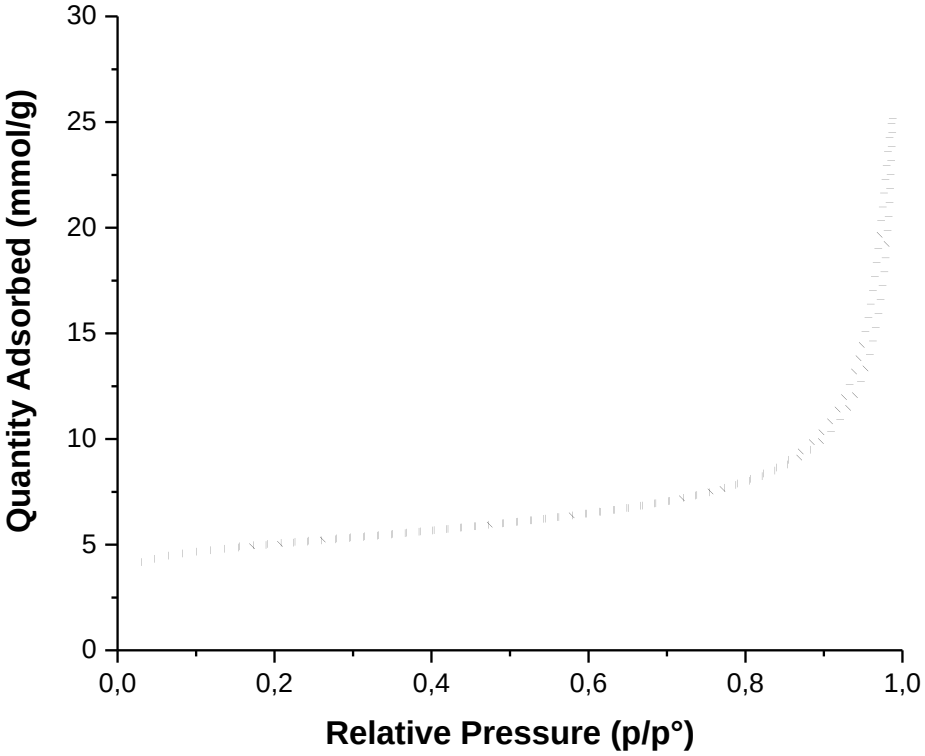

Figure 5.7 : N_2 adsorption/desorption isotherm at 77 K of pristine SWCNHs

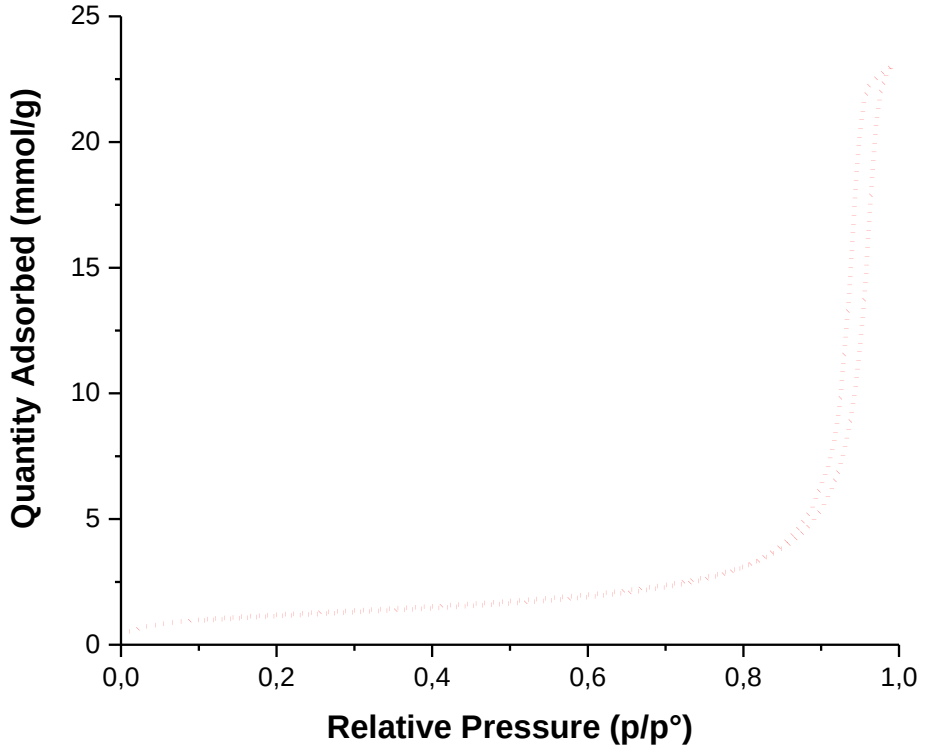

Figure 5.8 : N_2 adsorption/desorption isotherm at 77 K of **H1** material

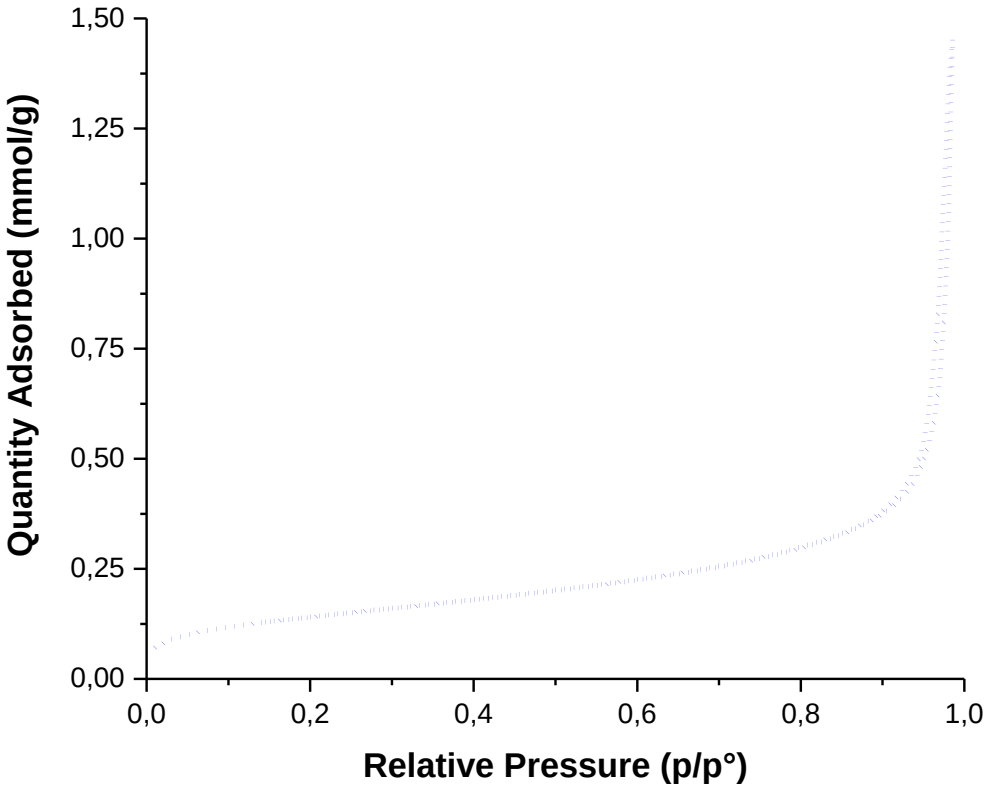

Figure 5.9 : N_2 adsorption/desorption isotherm at 77 K of **H2** material

The specific surface area of pristine SWCNHs was obtained by BET method and is equal to 358 $m^2.g^{-1}$. This value seem to be in accordance with literature [43,77]. In case of **H1** and **H2** (**Figure 5.8** and **Figure 5.9** respectively**)** N_2 adsorption/desorption gave nearly the same type of isotherm as in the pristine SWCNHs case, with nearly inexistent hysteresis in case of **H2** material.

Table 5.3 : Specific surface area of SWCNHs-based materials extracted from N_2 adsorption/desorption

Material	**SSA (BET)** ($m^2.g^{-1}$)
Pristine	358
H1	95
H2	11

Specific surface area estimation *via* BET method had shown the same tendency, as in case of carbon nanotubes-based catalysts (**Table 5.3**): the increase in amount of BV-Imi Br on the surface of the pristine nanostructure reduces its SSA. This difference is especially striking

between the SSA of pristine SWCNHs and **H2** material, where surface was reduced by a factor 32. This SSA decrease is most likely due to BV-Imi Br shell around dahlia-like nanohorn structure.

5.3.2. Second Method

In order to deepen investigations into SWCNHs-based catalysts a slightly different method was used to attach BV-Imi Br on the surface of carbon nanohorns, thus producing a series of catalysts called **H3**. The difference in the synthesis of this material comes from the difference in proportion of BV-Imi Br to SWCNHs. In this case, 1,88 mmol BV-Imi Br were used for 50 mg of SWCNHs. More details for this different synthesis method was explained in the experimental section.

H3 had the same series of analysis as previously mentioned SWCTHs- and SWCNHs-based catalyst. The only difference is situated in fact that the investigations for **H3** were led further compared to previously mentioned catalysts.

In first place, **H3** material was analysed with TEM (**Figure 5.10**). In comparison with pristine SWCNHs, **H3** is completely made of clusters containing dahlia flower-like structures coated in thick shell attributed to the presence of BV-Imi Br polymer. Some cluster reach dimensions of several micrometres, and the thickness of polymer shell may reach tens of nanometers in some clusters.

The amount of the BV-Imi Br in **H3** material was revealed by TGA and compared with **H1** and **H2** materials (**Figure 5.11**). The mass loss at 700 °C of **H3** is 66 %. From that value, it was possible once again to determine the amount of BV-Imi Br loaded on carbon nanohorns by using equation (4), and have the estimation of the amount of active species.

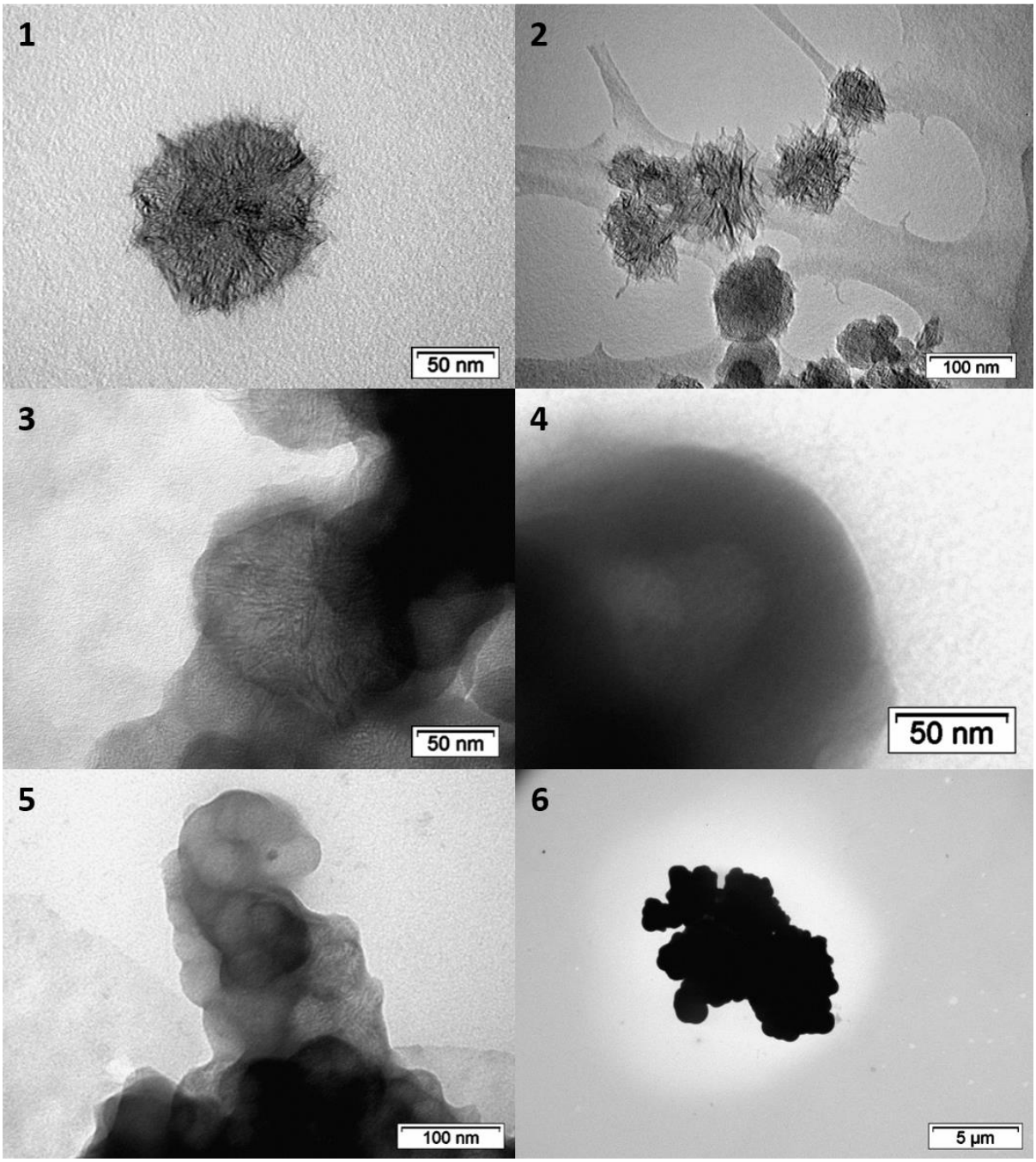

Figure 5.10 : TEM of pristine SWCNHs (1, 2) and of **H3** material (3-6) under different magnifications

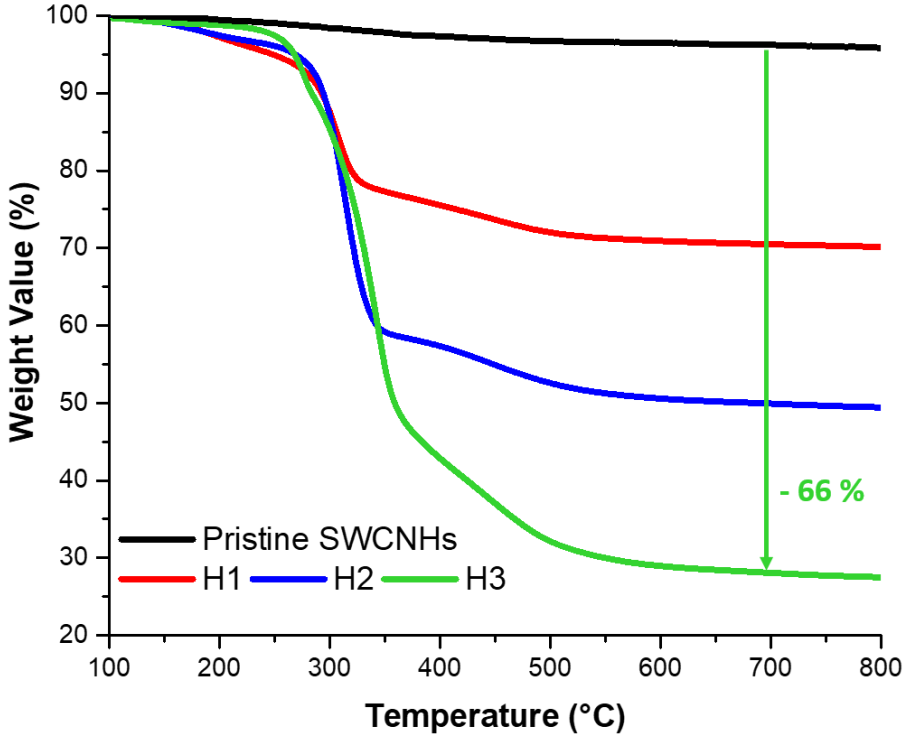

Figure 5.11 : TGA of pristine SWCNHs and SWCNHs-based materials, with **H3** derivative and its mass loss

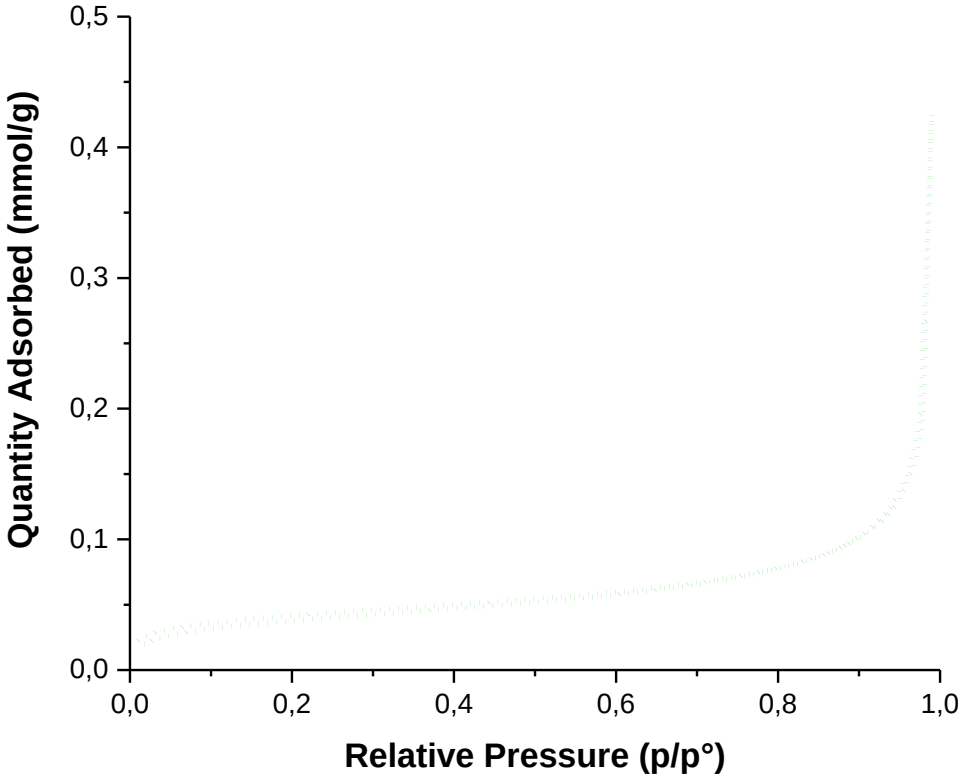

Figure 5.12 : N_2 adsorption/desorption isotherm at 77 K of **H3** material

Table 5.4 : Mass loss of **H1**, **H2**, **H3** and **T1**, **T2** materials, number of moles of BV-Imi Br ($n_{BV-Imi\ Br}$) calculated *via* equation (**5.2**), and number of moles of bromide (n_{Br-})

Material	Mass loss (%)	$n_{BV-Imi\ Br}$ (mmol.g^{-1})	n_{Br-} (mmol.g^{-1})
T1	23,58	0,52	1,04
T2	50,00	1,11	2,21
H1	23,28	0,51	1,03
H2	43,62	0,96	1,93
H3	65,80	1,46	2,91

The TGA of **H3** material (**Figure 5.11**) showed a weight loss of 65,80 %. This value was injected in equation (**5.1**) to obtain the number of moles of BV-Imi Br, and consequently the number of moles of active species – bromide. The amount of attached material was found to be even greater when compared to **H1**, **H2** and **T1**, **T2** materials due to the proportion of BV-Imi Br to the mass of SWCNHs used for the synthesis of **H3** material.

N_2 adsorption/desorption of **H3** material (**Figure 5.12**) had shown an isotherm (77 K) between Type II and Type III with no clear hysteresis, meaning presence of mesoporosity, as it was the case in **H1** and **H2** materials

5.4. Catalytic Tests

5.4.1. Bingel Cyclopropanation

The catalytic test performed with bin-mim-SWCNHs Br under conditions represented in **Scheme 5.2**.

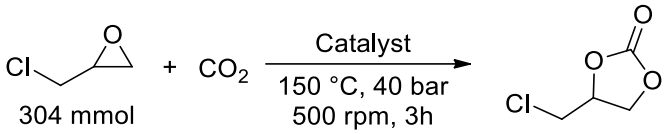

Scheme 5.2 : Synthesis of 4-chloromethyl-1,3-dioxolan-2-one from epichlorohydrin and CO_2 using Bin-Imi-SWCNHs Br as catalyst

The results for this catalytic test are represented as well as values needed TON as well as the values needed for its calculation are presented in **Table 5.5**. Despite fairly small amount of active species on the surface of the carbon nanohorns, the TON shows that the catalyst had an important influence on the studied reaction.

Table 5.5 : Conversion and TON of the Bin-Imi-SWCNHs Br material for the conversion of CO_2 and epichlorohydrin into 4-chloromethyl-1,3-dioxolan-2-one; 60 mg of material were used for this reaction

Catalyst	**Epichlorohydrin** (mmol)	**Conversion** (%)	**Br^- loading** ($mmol.g^{-1}$)	**TON**
Bin-Imi-SWCNHs Br	304	61,8	0,3	10400

Furthermore, the reuse tests were performed with Bin-Imi-SWCNHs Br. First catalytic test showed remarkable results conversion results with rather a small amount of active species. Unfortunately, the reuse of the Bin-Imi-SWCNHs Br, revealed itself unsuccessful. When the concerned catalyst was recovered after the first catalytic test, washed and reused under the same reaction conditions, it showed only traces of catalytic activity. Such drop in the conversion may be attributed to leaching of active species from the surface of the catalyst after the first run. The leaching might be explained either by the physisorption of the catalytic species on the surface of the pristine SWCNHs, or by the fact that the active species had undergone another chemical reaction – a reverse cyclopropanation due to the reaction conditions in the batch reactor.

5.4.2. H1, H2, H3 and T1, T2 materials

SWCNTs- and SWCNHs-based catalysts were compared by their catalytic activity. The experimental conditions of catalytic tests for each material are represented on **Scheme 5.3**, and the reaction outcome for each catalyst is summarized in **Table 5.6**.

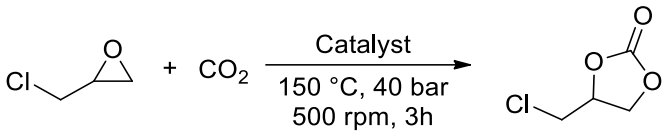

Scheme 5.3 : Synthesis of 4-chloromethyl-1,3-dioxolan-2-one from 304 mmol (28,13 g) of epichlorohydrin and CO_2 using 60 mg of catalyst (**T1**, **T2**, **H1**, **H2** or **H3**)

Table 5.6 : Conversion, TON and productivity for the **T1**, **T2**, **H1**, **H2**, **H3** materials used for the conversion of CO_2 and epichlorohydrin into 4-chloromethyl-1,3-dioxolan-2-one; 304 mmol (28,13 g) of epichlorohydrin and 60 mg per material were used for the catalytic tests

Material	**Br^- loading** ($mmol.g^{-1}$)	**Conversion** (%)	**TON**	**Productivity**
T1	1,06	40	1912	188
T2	2,21	69	1582	323
H1	0,97	44	2298	206
H2	1,95	74	1923	347
H3	2,91	80	1393	375

It appears that the SWCNHs-based catalysts seem to be more efficient for the conversion of CO_2 and epichlorohydrin, and have greater TON than their carbon nanotubes-based analogous, even though **T1** and **T2** catalysts have higher loading of active species. This results might be explained by better dispersion of **H1** and **H2** materials in reaction media.

Also, **H1** and **T1** catalysts have higher TON than **H2** and **T2** respectively, while having a lower conversion and productivity. Based on these results, the further attention was focused on **T2** and **H2** catalysts, since they showed better results in conversion and productivity after a 3 hours of reaction process.

Catalytic tests with epichlorohydrin revealed themselves very efficient in the synthesis of 4-(chloromethyl)-1,3-dioxolan-2-one. The decision was made to try **T2** and **H2** catalysts with another epoxide, since they have higher conversions and productivities, then recover and reuse concerned catalysts with the same epoxide. Styrene oxide was chosen for this purpose. The reaction conditions are represented on **Scheme 5.4**.

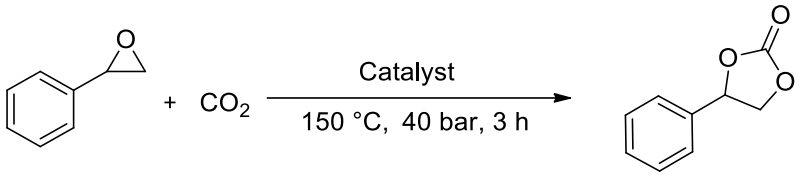

Scheme 5.4 : Synthesis of 4-phenyl-1,3-dioxolan-2-one from 202 mmol of styrene oxide and CO_2 in presence of either **T1**, **H2** or **H3** catalysts

Catalytic test with styrene oxide debuted with **T2** material. After the first run, the conversion of styrene oxide and CO_2 into 4-phenyl-1,3-dioxolan-2-one was of 24 % (**Table 5.7**).

Table 5.7 : Mass of the **T2** material, conversion of styrene oxide and CO_2 into 4-phenyl-1,3-dioxolan-2-one, TON and Productivity for **T2** material; molecular weight of styrene oxide is 120,15 $g.mol^{-1}$

Cycles	**T2** (mg)	**Styrene oxide** (mmol)	**Conversion** (%)	**TON**	**Productivity**
1	240	202	24	92	24
2	123	104	38	145	39

After the first cycle, 123 mg of **T2** catalyst were recovered, washed with MeOH, dried under vacuum at 60 °C, and reused. The recovered amount of **T2** was equal to 123 mg, thus the amount of styrene oxide had to be adapted. After the second cycle, the conversion became of 38 %. This result was surprising, as the expected conversion supposed to be equal or smaller compared to the first run. Also, if leaching had to take place, it had to happen during the first run, as it was the case of Bin-Imi-SWCNHs Br material. At the moment of the experiment there was no plausible explanation to this phenomenon, thus why would a catalytic activity of **T2** increase? It is important to mention, that the fact of keeping the same proportions between the

amounts of styrene oxide and the catalyst makes TON directly proportional to the conversion of reactants into product.

The reuse tests with styrene oxide was also performed with **H2** catalyst under the same experimental conditions that were used for **T2** catalyst. The first cycle of **H2** gave a conversion of 24 %, with TON equal to 104. The following cycles had shown an increase in conversion of reactants into product (**Figure 5.13**), as it was also the case of **T2** catalyst.

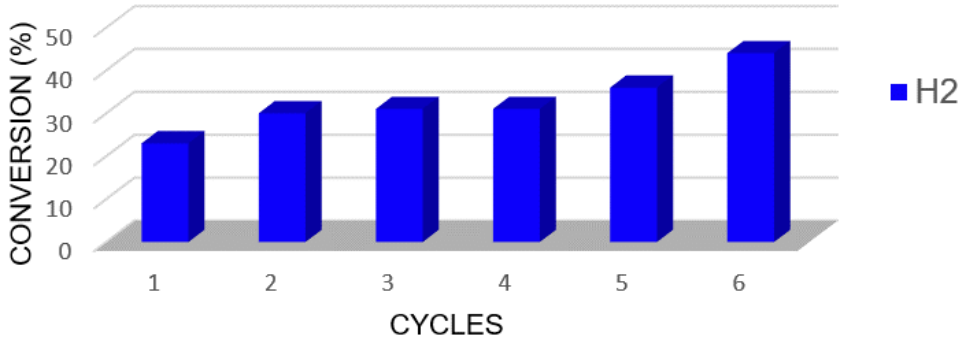

Figure 5.13 : Conversion for each reuse cycle of **H2** catalyst in the reaction between styrene oxide and CO_2

Possible explanation for this phenomenon was given in literature [38]: the reaction conditions might have an influence on the polymeric structure around SWCNHs. This structure is modified throughout the cycles, adapting itself and thus favouring the formation of 4-phenyl-1,3-dioxolan-2-one from styrene oxide and CO_2. In the literature, mercury porosimetry was used in order to show the difference between as called “fresh”, as synthetized catalyst and the one after the recycling tests. It appears that after several runs of reuse, the materials do increase their porosity, thus increasing surface are and catalytic activity proportionally.

Catalytic test for **H3** material were performed with epichlorohydrin (**Scheme 5.3**), and the results are summarized in **Table 5.6.** The conversion of CO_2 and epichlorohydrin into 4-chloromethyl-1,3-dioxolan-2-one as well as productivity are highest for **H3** among other materials after a reaction of three hours.

The reuse tests with **H3** material were made following reaction conditions described in **Scheme 5.4**. After each cycle **H3** catalyst was recover, washed with MeOH, dried in the vacuum oven at 60 °C and reused. Since the quantity of styrene oxide was adapted to the amount of **H3** used for the catalytic reaction, TON becomes directly proportional to the conversion of reactants into product. The catalyst was kept for a six cycles (**Figure 5.14**). The same tendency in **H3** reuse is observed as in case of **H2**: the conversion of reactants into product is increasing with each cycle, but the conversion is higher with each cycle in case of **H3**.

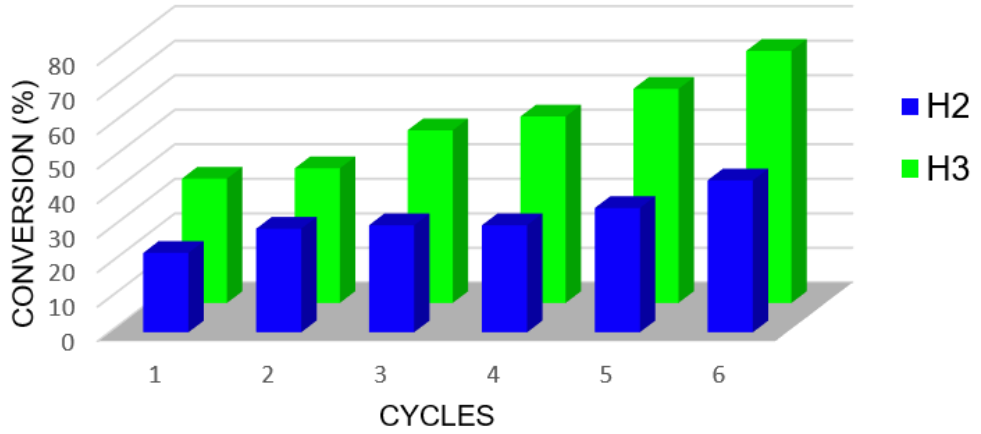

Figure 5.14 : Conversion for each reuse cycle of **H3** catalyst in the reaction between styrene oxide and CO_2

VI. CONCLUSIONS

Among the modification processes studied during this master thesis, the radical promoted attachment of BV-Imi Br on the surface of SWCNTs, or SWCNHs, through a radical promoted reaction revealed itself as a very easy and efficient way of making heterogeneous catalysts necessary for the conversion of CO_2 and epoxides into cyclic carbonates. In order to characterize novel materials, they were put through series of analytical techniques, such as TEM, TGA, N_2 adsorption/desorption. Information retrieved from these techniques allowed to visualize and compare the morphology of pristine, SWCNTs- and SWCNHs-based materials, to discover the amount of the active species linked to each material, and reveal the modification of the pore size distribution and specific surface are.

The comparison between catalytic activities of SWCNTs- and SWCNHs-based materials revealed slightly better performances for the carbon nanohorns-based catalysts. As a result, they were chosen for further investigations. In first place, the reuse of carbon nanohorns-based catalysts revealed a modification in the network of BV-Imi Br shell surrounding dahlia-like structure of CNHs. As a result, the activity of the catalyst was increased with each reuse. In second place, SWCNHs were used to try a faster synthesis method for the covalent grafting of BV-Imi Br, which revealed itself as a success. The material from new method revealed itself better either in simple catalytic tests, or in reuse, where it showed the similar, thus better tendencies in conversion with each step of reuse.

Novel SWCNHs-based materials were also used in tests with $ZnCl_2$ that played a role of a co-catalyst. Despite all expectations, $ZnCl_2$ revealed itself as an inhibitor of the active species for the concerned catalyst. On the other hand, EtOH used as a solvent for $ZnCl_2$, showed positive results for the conversion of reactants into product, thus acted as a co-catalyst. This might open new perspectives in the synthesis of BV-Imi-based heterogeneous catalysts.

VII. PERSPECTIVES

This master thesis, even though finished, still have a lot of potential experiments to be done. For instance, the attempt of the ionic exchange of the active species, thus bromide in BV-Imi Br, might be replaced simply by washing with KI salt, as iodide may also act as an active species and most likely have a better catalytic outcome [19].

Hydroxyl-functionalized ionic liquids have already been reported in literature and had showed interesting results in the conversion of CO_2 and epoxide into cyclic carbonate [31]. It would be interesting to investigate a way of integration of a Brønsted acid in the structure of a catalytic material. This modification could be performed on the surface of the catalyst, or integrated into homogeneous catalyst before the attachment on the surface of the catalytic support, or both modifications could be tried to be merged for an even greater outcome. The same idea may be applied to Lewis acid groups, since ZnX_2 species were reported to boost the conversion of CO_2 and epoxide.

Raman spectroscopy is an essential experimental tool. It might be used additionally for the characterization and comparison between pristine and functionalized carbon nanomaterials through the modifications of G- and D-bands in case of SWCNHs [41,78], and in case of SWCNHs [51]. Without having the possibility to use it during this master thesis, it would be great to use Raman to gather more information about synthetized heterogeneous catalysts.

VIII. EXPERIMENTAL PROCEDURES

8.1. Oxidation of Single Walled Carbon Nanohorns

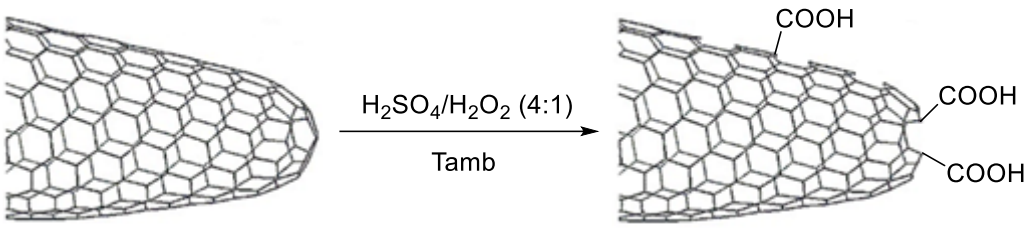

Scheme 1 : Oxidation of pristine SWCNHs with a Piranha solution

The piranha solution was made of 22 mL of H_2O_2 (30 %) added dropwise to 88 mL of H_2SO_4 at 0 °C and under agitation. Then, the mixture was added dropwise in a 250 mL round bottom flask containing 110 mg of SWCNHs with a magnetic stirrer. The mixture was left for 1 hour under agitation, filtered on a millipore filtering system, coated with a hydrophilic polyvinylidene fluoride (PVDF) millipore (0,1 µm) membrane filter, with a small volume of distilled water on top. The residue was washed with distilled water until pH was raised up to approximatively 6-7. The product was recovered with a millipore filtering system with an additional hydrophilic filter coating with a pore diameter of 0,1 µm, washed with 2x50 mL of MeOH and 2x50 mL of Et_2O. The black powder was then placed in a 100 mL round bottom flask, and sonicate for 5 minutes in 50 mL of methanol. The suspension was once again filtered on a millipore system with the same coating and washed with 50 mL of Et_2O. The recovered black powder was placed in a tared flask and was put it in a vacuum oven overnight. 121 mg of oxidized material (**Scheme 5**) had been recovered. It was characterized with TEM. [60]

8.2. Functionalization of Pristine SWCNHs *via* Bingel Cyclopropanation Reaction

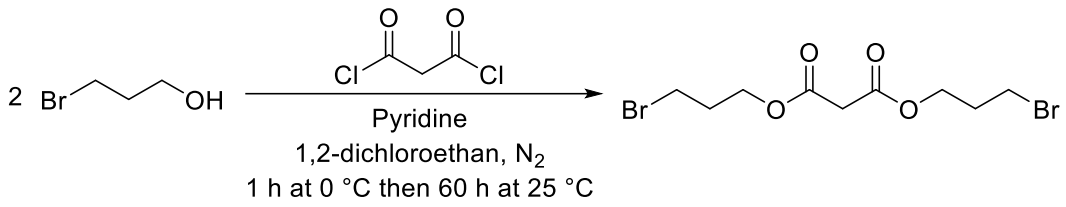

Scheme 2 : Synthesis of bis(3-bromopropyl) malonate

The functionalization of SWCNHs *via* Bingel reaction [64] was performed in three steps. The first step consisted in the synthesis of bis(3-bromopropyl) malonate (**Scheme 6**). In a two necked 50 mL round bottom flask with a magnetic stirrer under nitrogen at 0 °C, 9,7 mmol of 3-bromo-1-propanol were added to a solution of 9,9 mmol of anhydrous pyridine in 29,0 mL of anhydrous 1,2-dichloroethane (99,8 %). Next, 5,0 mmol of malonyl chloride were added. The reaction was left stirring at 0 °C for one hour, and at 25 °C for next 60 hours. Then, through decantation, the organic phase was recovered and washed with 160 mL of HCl (5 %), and with 200 mL of solution saturated with $NaHCO_3$. The aqueous phase was washed three times with 20 mL of CH_2Cl_2 and two organic fractions were brought together. The final product was recovered through short flash chromatography. The yield of the reaction was ~77 %, and the structure of the product was confirmed by ^{1}H-NMR.

^{1}H-NMR (400 MHz) in $CDCl_3$. δ: 2,20 (qui, J = 6,08; 6,36, 4H, CH_2*CH_2*-CH_2), 3,39 (s, 2H, CO-CH_2-CO), 3,45 (t, J = 6,48, 4H, CH_2-Br), 4,29 (t, J = 6,04, 4H, OCH_2).

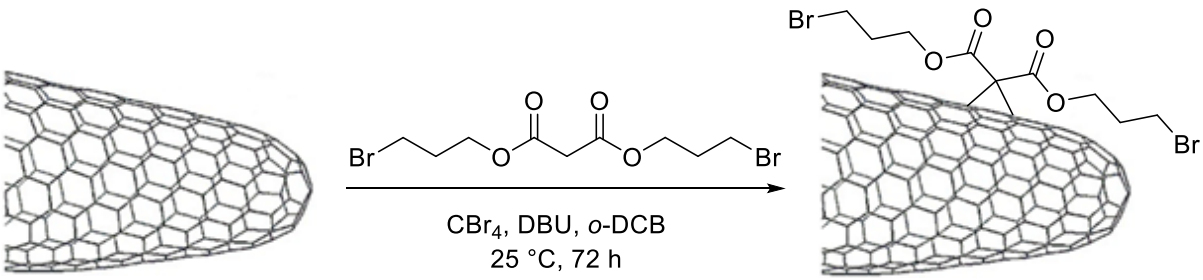

Scheme 3 : Covalent grafting of bis(3-bromopropyl) malonate on pristine SWCNHs *via* Bingel reaction

For the second step bis(3-bromopropyl) malonate was covalently attached onto the external surface of the pristine SWCNHs *via* Bingel reaction (**Scheme 7**). A solution of 100 mmol of CBr_4 (99%) in 32 mL of *o*-DCB was added to the suspension of 300 mg of pristine CNHs in 30 mL of *o*-DCB (99%). The volume was completed to 145 mL with *o*-DCB. The reaction started from the moment when 20 mmol of DBU were added. The reaction was left for 72 hours at 25 °C under magnetic stirring. Then, the reaction mixture was sonicated for 10 minutes, and a black powder was recovered through the filtering on a millipore system coated with a millipore membrane filter (PVDF, 0,1 µm). The black solid was washed with 2x50 mL of CH_2Cl_2, 5x50 mL of MeOH, 5x50 mL of H_2O milliQ, and finally with 2x50 mL of Et_2O. The black solid was once again recovered and was stocked in the vacuum oven at 60 °C overnight. Dried material was characterized by TGA.

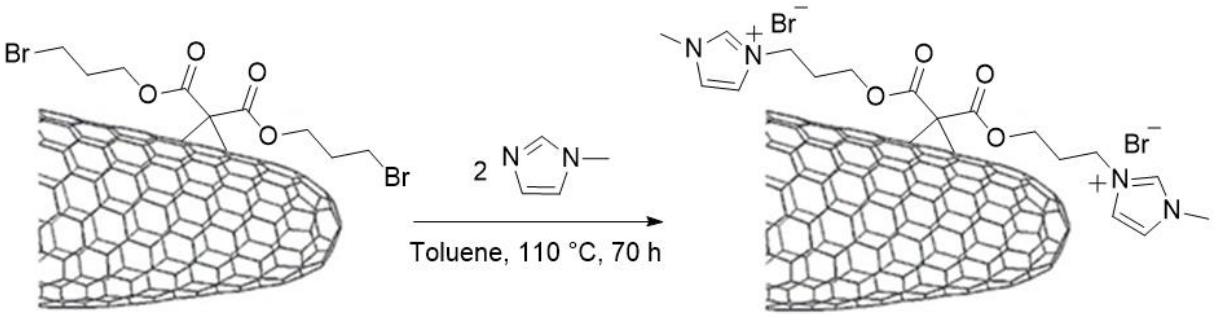

Scheme 4 : functionalization of bis(3-bromopropyl) malonate-CNHs with 1-methylimidazole

The third step of the experiment consisted of functionalization of bis(3-bromopropyl) malonate-SWCNHs with 1-methylimidazole (**Scheme 5**). A suspension of 323 mg bis(3-bromopropyl) malonate-SWCNHs in 50 mL of toluene was added into a 150 mL round bottom flask. Then, a solution of 25 mmol of 1-methylimidazole in 58 mL of toluene was added to the suspension. The system was closed, heated and the reaction was left for 70 hours at 110 °C under reflux. Then, the reaction mixture was cooled to room temperature, sonicated for 20 minutes and filtered on a millipore system coated with the millipore membrane filter (PVDF, 0,1 µm). The washing of the material required 2x20 mL of EtOAc and 2x20 mL of Et_2O. The black solid was recovered, sonicated for 10 minutes in 50 mL of toluene, filtered and washed again using the same amount of solvents. The black solid was recovered into a tared flask and put in a vacuum oven at 60 °C overnight. The dried black powder was submitted for TEM and TGA. This functionalized material will further in this work has the abbreviation bin-SWCNHs.

8.3. Synthesis of 1,4-bis(1-vinylimidazole-1-methylbenzene) bromide

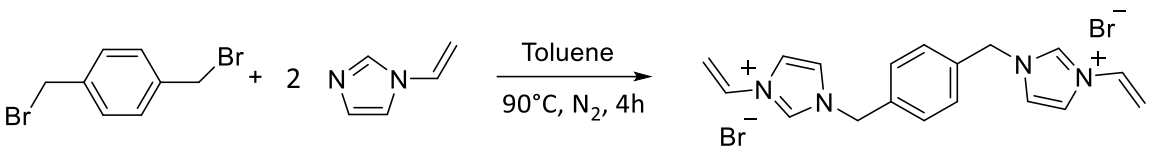

Scheme 5 : synthesis of 1,4-bis(1-vinylimidazole-1-methylbenzene) bromide from bromo-*para*-xylene and 1-vinylimidazole

11,03 mmol of bromo-*para*-xylene were placed in a two necked round bottom flask of 25 mL under N_2, and were covered with 10 mL of anhydrous toluene (99,8 %). The solution was heated up to 90 °C under magnetic steering. Then, 23,82 mmol of 1-vinylimidazole were added dropwise. The closed reaction system was left under N_2 and reflux for 4 hours. Afterwards, the system was cooled down to a room temperature. The mixture was filtered on the sintered glass funnel (Por. 4). The white residue was recovered and dissolved in 20 mL of hot MeOH. When the solution reached a room temperature, it was transferred into a beaker containing 100 mL of Et_2O. The mixture of the beaker was then filtered on sintered glass funnel (Por. 4), was cleaned with 2x20 mL of Et_2O, was recovered into a tared vial and was put in a vacuum oven at 60 °C overnight. The white solid was analysed by ^{1}H-NMR. The yield of the reaction was ~85 %.

^{1}H-NMR (400 MHz) in CD_3CN. δ: 5,36 (dd, 2H, J = 1,36; = 1,52, *cis*-CH=C**H**$_2$); 5,39 (s, 4H, C**H**$_2$Ph); 5,79 (dd, 2H, J = 2,56; = 15,64, *trans*-CH=C**H**$_2$); 7,21 (dd, 2H, J = 8,72; = 15,52; -C**H**=CH_2); 7,49 (complex, 4H Ph and 2H Imi); 7,69 (d, 2H Imi, J = 1,64); 9,37 (d, 2H, J = 1,16).

8.4. Functionalization of Pristine Carbon Nanostructures With Bis-Vinyl- imidazolium Bromide *via* Radical Polymerization

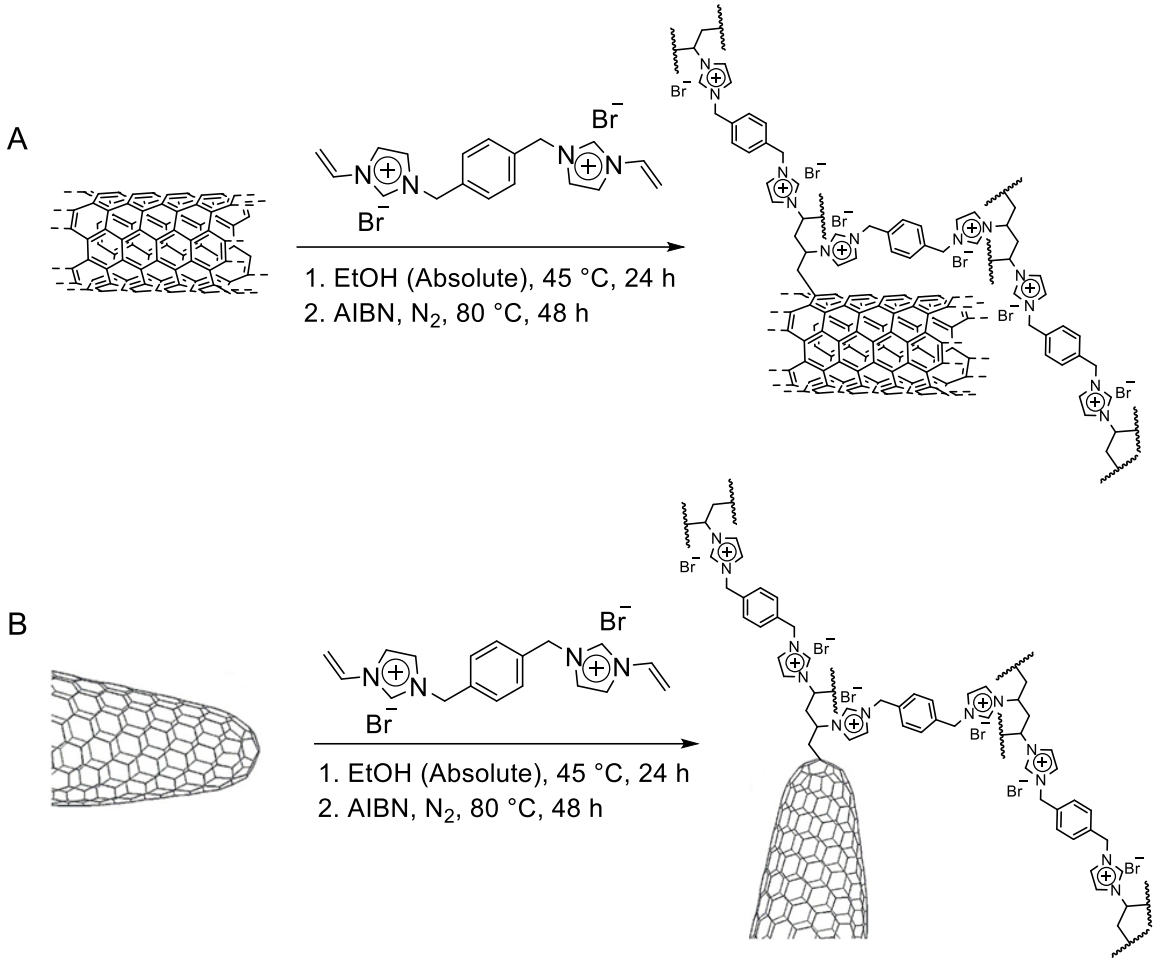

Scheme 6 : Heterogenization of BV-Imi Br on the surface of carbon nanomaterials: (**A**) – heterogenization on the surface of SWCNHs and (**B**) – on the surface of SWCNHs

The first functionalization of SWCNTs and SWCNHs with BV-Imi Br was prepared according to a procedure reported in the literature [37]. In two necked round bottom flask of 250 mL was added a solution of BV-Imi Br (2,13 mmol) and 150 mL of absolute EtOH. The system was heated to 45 °C and left under magnetic stirring until the complete dissolution of BV-Imi Br. Then, 130 mg of carbon nanomaterials were added into the solution. The system was closed and left at 45 °C under magnetic stirring for 24 h. Next, N_2 was bubbled for 10 min into the mixture. Next, the heating temperature was raised to 80 °C under reflux. The solution of AIBN (910 mmol) in 8 mL of absolute EtOH was added drop-wise under N_2 atmosphere. The reaction was left for 48 h. After cooling the reaction system to room temperature, the

reaction mixture was sonicated for 1 h and filtered through a millipore system, where a 0,45 μm PVDF membrane filter was used as a filtering system coating for SWCNTs, and 0,1 μm membrane filter (PVDF, 0,1 μm) for SWCNHs, until the disappearance of ionic liquid from filtrate. The recovered materials were placed in a round-bottom flask with 140 mL of MeOH and magnetically stirred at 60 °C overnight. Finally, the reaction products were filtered and dried under vacuum at 60 °C.

This method was used to synthetize two different batches of heterogeneous catalysts from each carbon nanostructure. The difference between those batches is the quantity of BV-Imi Br that was initially used for the synthesis of the catalysts (**Table 1**).

Table 1 : SWCNHs- and SWCNTs-based materials synthetized by the method adapted from the literature [1]; **T** and **H** stand for nanotubes and nanohorns respectively

Batch	**CNHs** (mg)	**BV-Imi Br** (mmol)	**Recovered Catalyst** (mg)
T1	130	1,06	195
T2	130	2,13	412
H1	130	1,06	177
H2	130	2,13	344

All the aforementioned products were analysed by TEM, TGA and N_2 adsorption/desorption method.

8.5. Advanced Functionalization of Pristine Single Walled Carbon Nanohorns With BV-Imi Br

This functionalization process used exclusively for SWCNHs is different from the previous by several reaction parameters, but most importantly it differs by the time it took to complete the reaction.

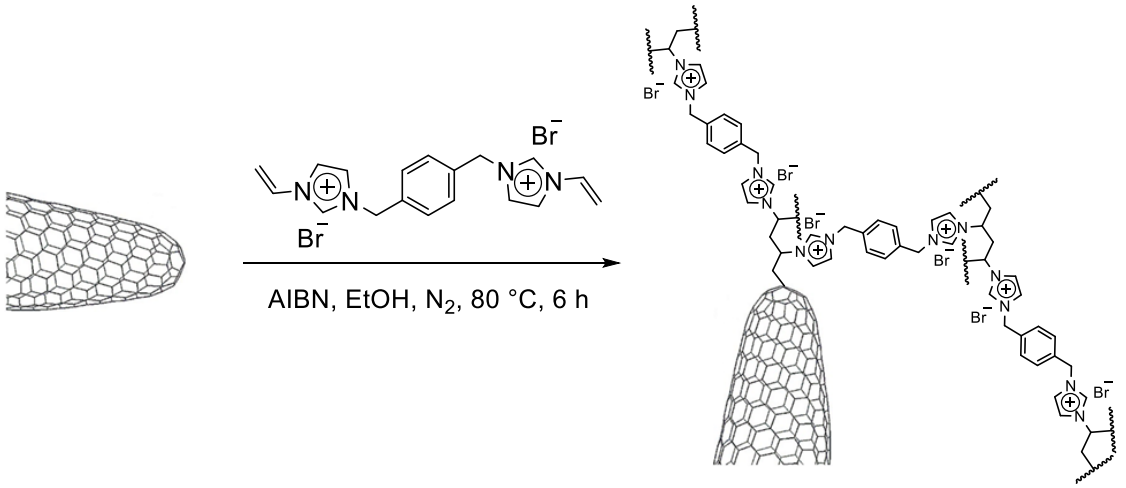

Scheme 7 : Heterogenization of BV-Imi Br on the surface of pristine-SWCNHs by a radical promoted reaction

The solution of 1,88 mmol of BV-Imi Br in 30 mL of absolute ethanol (99,8 %) was placed into a two necked round bottom flask of 50 mL with 50 mg of SWCNHs. The mixture was sonicated for 20 minutes. Then, N_2 was bubbled into the suspension for 10 minutes. Then, the system was heated up to 80 °C and 130 mmol of 2,2'-azobis(2-methylpropionitrile) (AIBN) were added. The reaction was left under N_2 atmosphere and magnetic stirring for 6 hours. Afterwards, the system was cooled down to a room temperature, the suspension was sonicated for 20 minutes, centrifuged for 10 minutes at 4500 rpm, and the recovered black solid was washed with MeOH. This was repeated until the complete elimination of physisorbed BV-Imi Br, which was verified by ^{1}H-NMR in CD_3OD. Then, the black powder was washed one last time with Et_2O and left in a vacuum oven overnight at 60 °C. The reaction product was checked through TEM, TGA and N_2 adsorption/desorption. The heterogeneous catalysts that came from this method were named **H3** by following the logic of the previous point.

8.6. Catalytic Tests

All the catalytic tests were performed on *Cambridge Bullfrog Batch Reactor* (**Picture 1).**

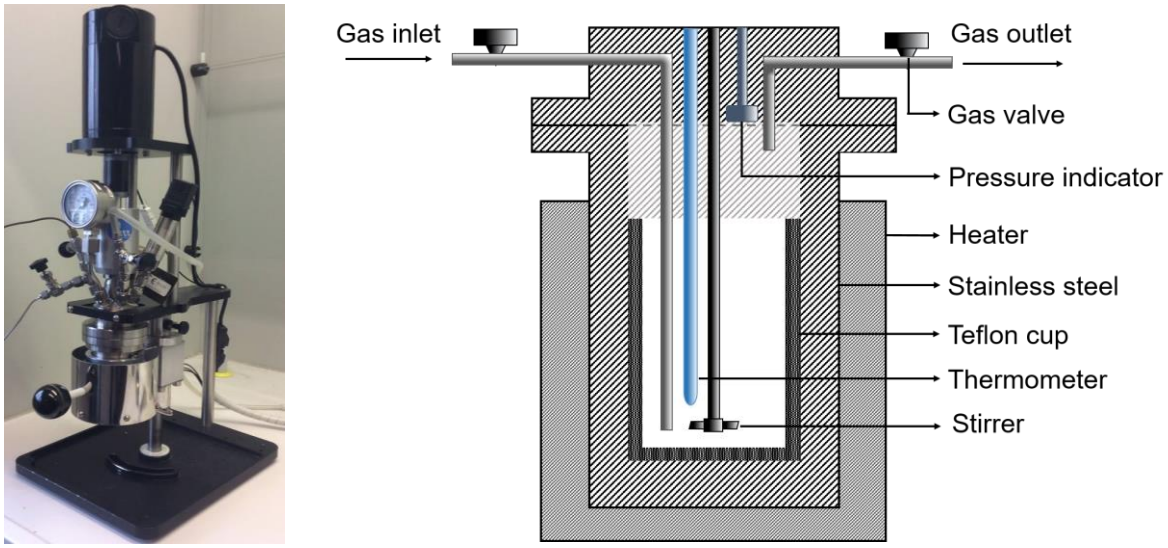

Picture 1 : picture of *Cambridge Bullfrog Batch Reactor* (left) and the approximate schematic representation of its reaction chamber (right)

Most of the catalytic tests did fall under the same experimental procedure (**Scheme 12**), unless specified differently further in this master thesis.

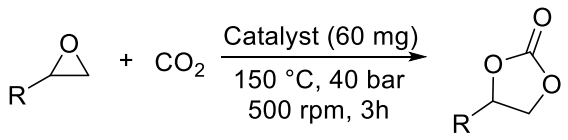

Scheme 8 : reaction conditions for the synthesis of five membered cyclic carbonates from a monosubstituted epoxides and CO_2

304 mmol of a monosubstituted epoxide were placed with 60 mg of heterogeneous catalyst in a glass vial. The suspension was sonicated for 10 minutes, then placed in the Teflon cup inside the reactor. The reactor was closed and sealed. The system was purged with N_2 under 4,5 bar for 10 minutes under a room temperature and under agitation at 500 rpm. Then, all the

N_2 was emptied from the system and replaced by 27 bar of CO_2. Then, when the pressure decreased to around 21 bar the heating of the reaction had begun. The countdown for the reaction started when the temperature of the mixture reached 150 °C. After 3 hours, the reaction was stopped, the reaction mixture was cooled down to 35 °C temperature, and was finally depressurized. The reaction mixture was recovered through 0,2 µm syringe filter and stored under -10 °C temperature.

The conversion of epoxide and CO_2 into a cyclic carbonate was verified by ^{1}H-NMR in $CDCl_3$.

Epichlorohydrin ^{1}H-NMR (400 MHz) in $CDCl_3$. δ: 2,66 (dd, 1 H, -C**H**$_2$Cl); 2,85 (t, 1 H, -C**H**$_2$Cl); 3,20 (m; 1 H, chiral); 3,49 (dd, 1 H, O-C**H**$_2$-CH); 3,61 (dd, 1 H, O-C**H**$_2$-CH).

4-(chloromethyl)-1,3-dioxolan-2-one ^{1}H-NMR (400 MHz) in $CDCl_3$. δ: 3,71 (dd, 1 H, O-C**H**$_2$-CH); 3,80(dd, 1 H, O-C**H**$_2$-CH), 4,37 (dd, 1 H, -C**H**$_2$Cl); 4,56 (t, 1 H, -C**H**$_2$Cl); 4,98 (m; 1 H, chiral).

Styrene oxide ^{1}H-NMR (400 MHz) in $CDCl_3$. δ: 2,80 (dd, 1 H, C**H**$_2$-O); 3,14 (dd, 1 H, C**H**$_2$-O); 3,86 (dd, 1 H, Ph-C**H**); 7,34 (m, 5 H, Ph).

4-phenyl-1,3-dioxolan-2-one ^{1}H-NMR (400 MHz) in $CDCl_3$. δ: 4,31(dd, 1 H, C**H**$_2$-O); 4,76 (dd, 1 H, C**H**$_2$-O); 5,64 (t, 1 H, Ph-C**H**); 7,34 (m, 5 H, Ph).

IX. CHARACTERIZATION TECHNIQUES

In this section will be described characterisations techniques that were used to characterize materials synthetized during this master thesis.

9.1. Nitrogen adsorption/desorption

N_2 adsorption/desorption is a characterisation technique elaborated to study physical properties of porous solids and fine powders. It is based on the physisorption of gaseous molecules on the surface of solid materials. The most commonly used gas for the adsorption on the surface of a sample is nitrogen.

The experimental protocol is divided into 4 steps:

- Sample outgassing;
- Dead space volume calibration;
- Adsorption;
- Desorption;

The outcome of this steps is an isotherm of characterized material. It gives the information about the surface of characterized material, it's porosity, as well as the affinity of the gas for the surface of the solid. Isotherms are classified into 6 types by IUPAC (**Figure 9.1**). Thus, Type I isotherms are characteristic of microporous materials with limited uptake due to the accessible micropore volume. Types II and III are characteristic of nonporous or macroporous materials where "Point B" usually represents a completion of monolayer coverage. Type IV isotherms are obtained from mesoporous martials where gas condensation takes place inside of the pores. Type V are characteristic of water adsorption on hydrophobic microporous and mesoporous materials, and Type VI isotherms appears in case of a layer by layer adsorption of gas on uniform nonporous surface. [76]

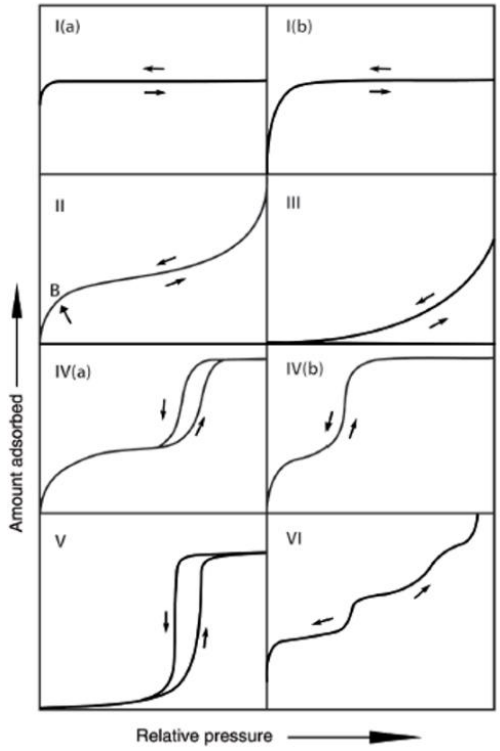

Figure 9.1 : IUPAC classification of physisorption isotherms (adapted from [76])

The surface between adsorption and desorption curves is called hysteresis loop. The origin of this loop is attributed to capillary condensation, and is related to pore structure, as well as the adsorption mechanisms. The most representative loops are shown on **Figure 9.2**.

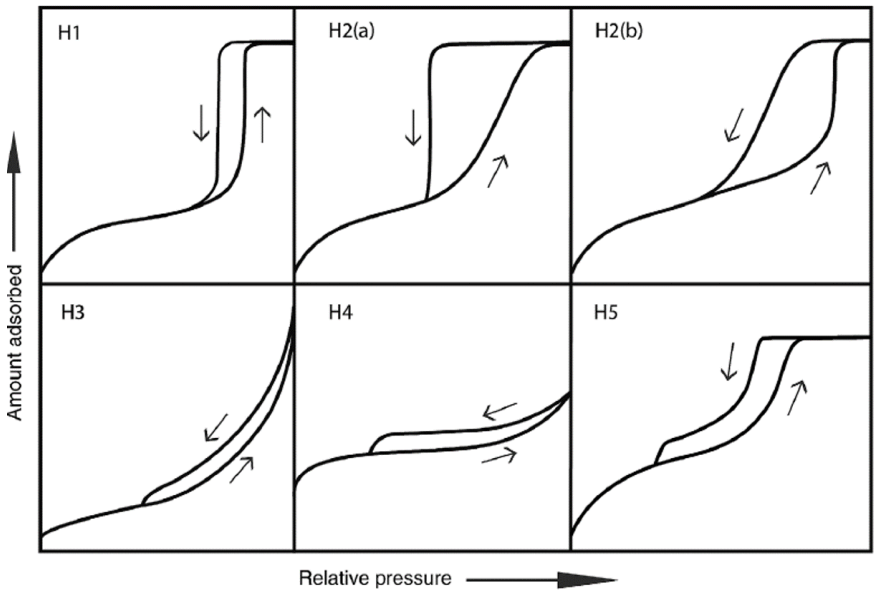

Figure 9.2 : IUPAC classification of hysteresis loops (adapted from [76])

Type *H1* hysteresis is often attributed to the materials with uniform structured mesopores, like in template silicas such as SBA-15 or MCM-41, pore glasses and ordered mesoporous carbons. Type *H2* loops are given by materials with complex pore structure, in which pore-blocking or cavitation-induced evaporation are possible. The difference between *H2a* and *H2b* hysteresis comes from the difference in the shape of pores. Type *H3* hysteresis is significant of large pores which are partially filled with condensate. Type *H4* hysteresis is typical of micro-mesoporous carbons, aggregated crystals of zeolites, and some mesoporous zeolites. Type *5* loop is attributed to mesoporous materials with both opened and partially blocked pores.

Furthermore, it is possible to extract specific surface area from isotherm using Brunauer–Emmett–Teller method. To use this method, following assumptions should be taken in consideration [75]:

- The surface of the material has to be homogeneous;
- There is an equilibrium between the adsorption and desorption of molecules;
- Adsorbed molecules can form several layers;
- First layer is different from all following layers;
- Second and following layers are considered to have same characteristics as the bulk fluid phase;
- There are no lateral interactions between adsorbed layers;

The obtained physisorption isotherm is transformed into a "BET plot" in order to obtain the BET monolayer capacity, n_m. Thus, the BET equation is applied to the linear plot (**9.1**):

$$\frac{p/p^\circ}{n(1-p/p^\circ)} = \frac{1}{n_m C} + \frac{C-1}{n_m C}(p/p^\circ) \qquad (\mathbf{9.1})$$

where p and $p°$ are the equilibrium and the saturation pressure of adsorbates at the temperature of adsorption, n is the adsorbed gas quantity, n_m is specific monolayer capacity, and C is the constant related to the energy of the monolayer adsorption.

Furthermore, knowing n_m, BET specific surface area can be calculated (**9.2**):

$$SSA_{BET} = n_m . \sigma_m . N_A / V_M \quad \textbf{(9.2)}$$

where SSA_{BET} is specific surface area obtained by BET method, σ_m is a molecular cross-section area, N_A is Avogadro's Number and V_M is a molar volume of the adsorbate gas. [75,76]

In this master thesis, the samples characterized by nitrogen adsorption/desorption were either SWCNHs-based, or SWCNTs-based materials. All the physisorption experiments were performed on Micrometics TriStar 3000 with N_2 at -196 °C (boiling point of N_2). Before the characterization, all of the materials were outgassed under vacuum (0.1 mbar) at 120 °C overnight with Micrometrics VacPrep 061.

9.2. Nuclear Magnetic Resonance Spectroscopy

The importance of the NMR in chemistry comes from the fact that the signals are isotope-specific, and can be attributed to a particular chemical element and nuclide. This type of spectroscopy is based around the interpretation of chemical shift phenomena. This shift refers to a difference in resonance frequency (equation **9.3**) between nuclei in different chemical sites. Such nuclei behaviour depends on its electronic environment that causes the variation of in shielding.

$$\nu = \frac{\gamma}{2\pi} B_0(1 - \sigma) \qquad (\mathbf{9.3})$$

In this equation the resonance frequency (ν) is proportional to the strength of the static magnetic field (B_0), as well as to the magnetogyric ratio of the nucleus (γ), and shielding constant (σ) [79]. Chemical shift of X atom can be defined as resonance of different X atoms at different frequencies [80]. In order to make chemical shifts values ($\delta_{X,sample}$) comparable, they were referenced to a standard such as tetramethylsilane (equation **9.4**) [75].

$$\delta_{X,sample} = \left(\frac{\nu_{X,sample} - \nu_{X,reference}}{\nu_{X,reference}}\right).10^6$$

Protons are very sensible to the ^{1}H-NMR spectroscopy because it has high magnetogyric ratio and it is usually very abundant in molecules. Inside a molecule, protons may interact one with another due to their proximity. This phenomenon is called proton coupling. It allows to look at the way the C-H skeleton is assembled. If two protons, located on two different carbon atoms, are close to each other, they will perceive not only the applied magnetic field, B_0, but also the magnetic field of their neighbour. This results in a split of a signal in the spectrum for both protons. This split is called coupling constant, J (Hz), and it measures the interaction between a pair of protons. This constant can be determined from the ^{1}H-NMR spectrum and converted in Hz (equation **9.5**) since NMR spectra are in parts per million (ppm).

$$J = (\Delta peak. R_{NMR}). 10^{-6} \quad \textbf{(9.5)}$$

$\Delta peak$ stands for the difference in ppm between two peaks of a signal and R_{NMR} is the rating of the NMR machine (MHz). The splitting of a signal depends on the number n of protons located on neighbouring carbon atoms, and gives $n + 1$ lines as a result. If there are several protons on one carbon atoms, they are called equivalent since they don't interact one with another [81].

^{1}H-NMR spectra were made on liquid-state 400 MHz Jeol ECX with 5-mm direct broadband probe.

9.3. Thermogravimetric Analysis

TGA is one of the thermal methods of investigations used to observe the mass variation of a sample versus temperature in controlled atmosphere. This technique reveal itself very useful in the reactions related to a mass loss, or a mass gain especially interesting for the solid-gas systems. It can be also used to observe the physical changes in the solid samples such as a phase transition.

The instrument is composed of a crucible connected to a balance. The crucible is inserted into a furnace with control over the atmosphere. Crucible may be mad of diverse materials, and adapted to the experimental conditions. The furnace must have a high temperature resistance as well as the possibility to have a controlled atmosphere which leads to a possibility to performed an important number of different experiments. The is the key element of the thermogravimeter. It is based on the "zero method" principle where the mobile part is kept stable, and the compensating force is registered as a signal. [75]

In this work, TGA was used to measure a weight loss of the synthetized materials and compare it to pristine carbon nanostructures, either SWCNHs or SWCNTs. The obtained weight loss values allowed to obtain the loading of the active species for each material. The performed under nitrogen flow from 100 to 1000°C with a heating rate of 10 °C/min in a Mettler Toledo TGA STAR system.

9.4. Transmission Electron Microscopy

The electron microscopes are optical systems that allow to observe a small size samples under a high magnification that can be tuned between 10^3 and 10^6 times, and are able to resolve distances down to 18 nanometers. Those microscopes use incident high energy electron beam that interacts with the matter to probe a sample. This interaction causes the series of different phenomena illustrated on **Figure 9.3**.

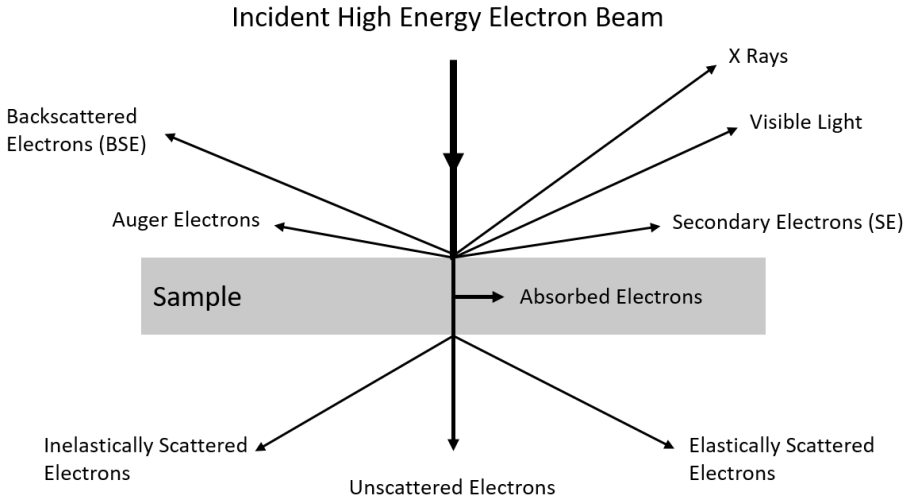

Figure 9.3 : Schematic representation of high energy electron beam interacting with matter

In case of TEM, the electrons that have been scattered in the forward direction (unscattered, inelastically and elastically scattered electrons) are collected and transformed into an image of the sample.

The functioning principle of transmission electron microscope starts with the emission of the high energy electron beam directed to the sample (**Figure 9.4**). The electrons are generated by a heated filament of tungsten or lanthanide hexaboride on the top of the microscope. Throughout the beam path, the electrons travel in high vacuum through a series of electromagnetic lenses needed to direct and to focus the beam. When in interaction with the sample, the scattering of the electrons is proportional to the density of the sample. The electrons that were scattered the most will give darker shade on the final image. After the sample, the

electron beam will once more pass through a series of amplifying lenses to be finally projected on the fluorescent screen or to be captured by a specially adapted camera. The obtained images are in black and white reveal the morphology of studied sample through its cross section. [75]

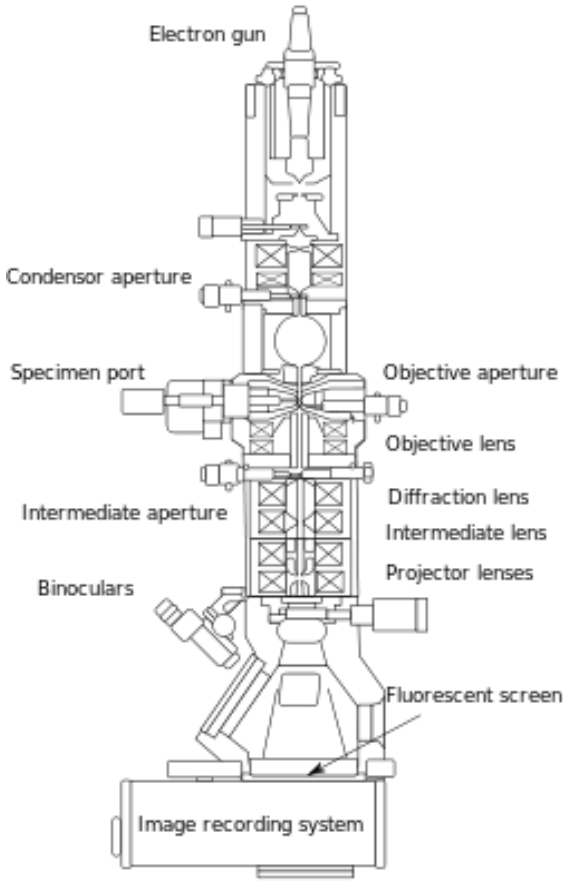

Figure 9.4 : Schematic representation of high energy electron beam interacting with matter (Wikipedia)

In this master thesis, the TEM images were recorded on a Philips TECNAI 10 at 80-100 kV. The preparation of the samples required the sonication of the synthetized materials in absolute ethanol for 15 minutes. Three droplets of the suspension were then deposited on *Formvar-coated copper grid*, dried and inserted into the specimen port. The program used for the picture management is ImageJ.

X. BIBLIOGRAPHY

[1] S.A. Montzka, E.J. Dlugokencky, J.H. Butler, *Nature*, **2011**, *476*, 43

[2] A. Raval, V. Ramanathan, *Nature*, **1989**, *342*, 758

[3] M. Qiancheng, NASA GISS: Science Briefs: Greenhouse Gases: Refining the Role of Carbon Dioxide. *Greenhouse Gases: Refining the Role of Carbon Dioxide*, 1998

[4] A.A. Lacis, G.A. Schmidt, D. Rind, R.A. Ruedy, *Science*, **2010**, *330*, 356

[5] IPCC, Climate Change 2014: Mitigation of Climate Change. *Working Group III Contribution to the Fifth Assessment Report of the Intergovernmental Panel on Climate Change*, 2014

[6] L. Hughes, *Trends in Ecology & Evolution*, **2000**, *15*, 56

[7] *IPCC report*, **2005**

[8] R. Steeneveldt, B. Berger, T.A. Torp, *Chemical Engineering Research and Design*, **2006**, *84*, 739

[9] E.S. Rubin, C. Chen, A.B. Rao, *Energy Policy*, **2007**, *35*, 4444

[10] E.S. Rubin, J.E. Davison, H.J. Herzog, *International Journal of Greenhouse Gas Control*, **2015**, *40*, 378

[11] M. Aresta, A. Dibenedetto, A. Angelini, *Chemical Reviews*, **2014**, *114*, 1709

[12] E.J. Beckman, *Nature*, **2016**, *531*, 180

[13] T. Sakakura, J.C. Choi, H. Yasuda, *Chemical Reviews*, **2007**, *107*, 2365

[14] A.-A.G. Shaikh, S. Sivaram, *Chemical Reviews*, **1996**, *96*, 951

[15] J.H. Clements, *Industrial & Engineering Chemistry Research*, **2003**, *42*, 663

[16] S. Fukuoka, M. Kawamura, K. Komiya, M. Tojo, H. Hachiya, *et al.*, *Green Chemistry*, **2003**, *5*, 497

[17] B. Schäffner, F. Schäffner, S.P. Verevkin, A. Börner, *Chemical Reviews*, **2010**, *110*, 4554

[18] T. Sakakura, K. Kohno, *Chemical Communications*, **2009**, 1312

[19] M. North, R. Pasquale, C. Young, *Green Chemistry*, **2010**, *12*, 1514

[20] S. Enyedi, *2018 IEEE International Conference on Automation, Quality and Testing, Robotics (AQTR)*, **2018**, 1

[21] P. Hertzke, N. Müller, S. Schenk, T. Wu, *McKinsey Centre for Future Mobility*, **2018**, 1

[22] P. Atkins, J. Paula, Physical chemistry. *W.H. Freeman*, 2010

[23] F. Cavani, F. Trifiró, *Catalysis Today*, **1997**, *34*, 269

[24] H. Nur, **2007**, *3*, 1

[25] T. Welton, *Chemical Reviews*, **1999**, *99*, 2071

[26] S. Zhang, N. Sun, X. He, X. Lu, X. Zhang, *Journal of Physical and Chemical Reference Data*, **2006**, *35*, 1475

[27] R.D. Rogers, *Science*, **2003**, *302*, 792

[28] F. Jutz, J.-M. Andanson, A. Baiker, *Chemical Reviews*, **2010**, *111*, 322

[29] V. Caló, A. Nacci, A. Monopoli, A. Fanizzi, *Organic Letters*, **2002**, *4*, 2561

[30] J. Sun, S.I. Fujita, M. Arai, *Journal of Organometallic Chemistry*, **2005**, *690*, 3490

[31] J. Sun, S. Zhang, W. Cheng, J. Ren, *Tetrahedron Letters*, **2008**, *49*, 3588

[32] L. Xiao, D. Su, C. Yue, W. Wu, *Journal of CO2 Utilization*, **2014**, *6*, 1

[33] P.P. Pescarmona, M. Taherimehr, *Catalysis Science & Technology*, **2012**, *2*, 2169

[34] Z.-Z. Yang, Y.-N. Zhao, L.-N. He, *RSC Advances*, **2011**, *1*, 545

[35] V.C. Raghunath, "Heterogenized Homogeneous Catalysts for Fine Chemicals Production: Materials and Processes". *Platinum Metals Review*, 2011, *55*

[36] Y. Zhang, S. Yin, S. Luo, C.T. Au, *Industrial and Engineering Chemistry Research*, **2012**, *51*, 3951

[37] M. Buaki-Sogó, A. Vivian, L.A. Bivona, H. García, M. Gruttadauria, C. Aprile, *Catal. Sci. Technol.*, **2016**, *6*, 8418

[38] C. Calabrese, L.F. Liotta, E. Carbonell, F. Giacalone, M. Gruttadauria, C. Aprile, *ChemSusChem*, **2017**, *10*, 1202

[39] S. Iijima, M. Yudasaka, *Chemical Physics Letters*, **1999**, *309*, 165

[40] M. Yudasaka, S. Iijima, V.H. Crespi, *Growth Lakeland*, **2008**, *629*, 605

[41] N. Karousis, I. Suarez-Martinez, C.P. Ewels, N. Tagmatarchis, *Chemical Reviews*, **2016**, [submitted]

[42] S. Utsumi, H. Honda, Y. Hattori, H. Kanoh, K. Takahashi, *et al.*, *Journal of Physical Chemistry C*, **2007**, *111*, 5572

[43] S. Zhu, G. Xu, *Nanoscale*, **2010**, *2*, 2538

[44] D.M. Guldi, **2007**, 1400

[45] J. Miyawaki, M. Yudasaka, T. Azami, Y. Kubo, S. Iijima, *ACS Nano*, **2008**, *2*, 213

[46] S. Iijima, *Nature*, **1991**, *354*, 56

[47] S. Iijima, T. Ichihashi, *Nature*, **1993**, *363*, 603

[48] A. Eatemadi, H. Daraee, H. Karimkhanloo, M. Kouhi, N. Zarghami, *Nanoscale Research Letters*, **2014**, *9(1)*, 1

[49] M. Terrones, *International Materials Reviews*, **2004**, *49*, 325

[50] M. Cinke, M. Cinke, J. Li, J. Li, B. Chen, *et al.*, *Chemical Physics Letters*, **2002**, *365*, 69

[51] C. Herrero-Latorre, J. Álvarez-Méndez, J. Barciela-García, S. García-Martín, R.M. Peña-Crecente, *Analytica Chimica Acta*, **2015**, *853*, 77

[52] P. Ajayan, O. Zhou, **2001**, *80*, 391

[53] M.F.L. De Volder, S.H. Tawfick, R.H. Baughman, A.J. Hart, *Science*, **2013**, *339*, 535

[54] F. Kreupl, A.P. Graham, G.S. Duesberg, W. Steinhögl, M. Liebau, *et al.*, *Microelectronic Engineering*, **2002**, *64*, 399

[55] A. Bianco, K. Kostarelos, M. Prato, *Current Opinion in Chemical Biology*, **2005**, *9*, 674

[56] P. Serp, M. Corrias, P. Kalck, *Applied Catalysis A: General*, **2003**, *253*, 337

[57] P. Agrigento, S.M. Al-Amsyar, B. Sorée, M. Taherimehr, M. Gruttadauria, *et al.*, *Catalysis Science & Technology*, **2014**, *4*, 1598

[58] L.A. Bivona, O. Fichera, L. Fusaro, F. Giacalone, M. Buaki-Sogo, *et al.*, *Catal. Sci. Technol.*, **2015**, *5*, 5000

[59] C. Cioffi, S. Campidelli, C. Sooambar, M. Marcaccio, G. Marcolongo, *et al.*, *Journal of the American Chemical Society*, **2007**, *129*, 3938

[60] N. Karousis, T. Ichihashi, S. Chen, H. Shinohara, M. Yudasaka, *et al.*, *Journal of Materials Chemistry*, **2010**, *20*, 2959

[61] V. Campisciano, V. La Parola, L.F. Liotta, F. Giacalone, M. Gruttadauria, *Chemistry - A European Journal*, **2015**, *21*, 3327

[62] R. Yuge, T. Ichihashi, Y. Shimakawa, Y. Kubo, M. Yudasaka, S. Iijima, *Advanced Materials*, **2004**, *16*, 1420

[63] M. Zhang, M. Yudasaka, K. Ajima, J. Miyawaki, S. Iijima, *ACS Nano*, **2007**, *1*, 265

[64] C. Bingel, *Chem. Ber.*, **1993**, *126*, 1957

[65] K.S. Coleman, S.R. Bailey, S. Fogden, M.L.H. Green, *Journal of the American Chemical Society*, **2003**, *125*, 8722

[66] T. Umeyama, N. Tezuka, M. Fujita, Y. Matano, N. Takeda, *et al.*, *Journal of Physical Chemistry C*, **2007**, *111*, 9734

[67] C.K. Chua, M. Pumera, *Chemical Society Reviews*, **2013**, *42*, 3222

[68] L. Jin, T. Liu, *Journal of Macromolecular Science, Part A: Pure and Applied Chemistry*, **2016**, *53*, 433

[69] S.P. Economopoulos, G. Pagona, M. Yudasaka, S. Iijima, N. Tagmatarchis, *Journal of Materials Chemistry*, **2009**, *19*, 7326

[70] H. Richter, M. Treska, J.B. Howard, J.Z. Wen, S.B. Thomasson, *et al.*, *Journal of nanoscience and nanotechnology*, **2008**, *8*, 6065

[71] G. Widmann, *UserCom*, **2001**, 1

[72] K.S.W. Sing, *Pure and Applied Chemistry*, **1985**, *57*, 603

[73] F. Li, Y. Wang, D. Wang, F. Wei, *Carbon*, **2004**, *42*, 2375

[74] Z.A. Alothman, *Materials*, **2012**, *5*, 2874

[75] M. Che, J. C. Vedrine, Characterization of Solid Materials and Heterogeneous Catalysts. Wiley-VCH Verlag & Co. KGaA, 2012

[76] M. Thommes, K. Kaneko, A. V. Neimark, J.P. Olivier, F. Rodriguez-Reinoso, *et al.*, *Pure and Applied Chemistry*, **2015**, *87*, 1051

[77] K. Murata, K. Kaneko, F. Kokai, K. Takahashi, M. Yudasaka, S. Iijima, *Chemical Physics Letters*, **2000**, *331*, 14

[78] G. Pagona, G. Mountrichas, G. Rotas, N. Karousis, S. Pispas, N. Tagmatarchis, *International Journal of Nanotechnology*, **2009**, *6*, 176

[79] R.K. Harris, E.D. Becker, S.M. Cabral de Menezes, R. Goodfellow, P. Granger, *Pure and Applied Chemistry*, **2001**, *73*, 1795

[80] M. Balci, in Elsevier Science, 2005, 430

[81] J. Clayden, G. Nick, W. Stuart, Organic chemistry (2nd edition). Oxford University Press, 2012